The Cerebellum (2019) 18:615–634
https://doi.org/10.1007/s12311-019-01017-5

REVIEW

Motor Performances of Spontaneous and Genetically Modified Mutants with Cerebellar Atrophy

Robert Lalonde[1] · Catherine Strazielle[2]

Published online: 28 February 2019

Abstract

Chance discovery of spontaneous mutants with atrophy of the cerebellar cortex has unearthed genes involved in optimizing motor coordination. Rotorod, stationary beam, and suspended wire tests are useful in delineating behavioral phenotypes of spontaneous mutants with cerebellar atrophy such as *Grid2*^{Lc}, *Grid2*^{ho}, *Rora*^{sg}, *Agtpbp1*^{pcd}, *Reln*^{rl}, and *Dab1*^{scm}. Likewise, transgenic or null mutants serving as experimental models of spinocerebellar ataxia (SCA) are phenotyped with the same tests. Among experimental models of autosomal dominant SCA, rotorod deficits were reported in SCA1 to 3, SCA5 to 8, SCA14, SCA17, and SCA27 and stationary beam deficits in SCA1 to 3, SCA5, SCA6, SCA13, SCA17, and SCA27. Beam tests are sensitive to experimental therapies of various kinds including molecules affecting glutamate signaling, mesenchymal stem cells, anti-oligomer antibodies, lentiviral vectors carrying genes, interfering RNAs, or neurotrophic factors, and interbreeding with other mutants.

Keywords Cerebellum · Purkinje cells · Rotorod · Stationary beam · Wire suspension · Spinocerebellar ataxia

Introduction

Naturally mutated mice with cerebellar atrophy have been known for over half a century [1, 2]. Over the course of the last quarter century, technological advances in transgenic and targeted null mutations have yielded genetically modified mutants with cerebellar atrophy, notably to model autosomal dominant spinocerebellar ataxias (SCAs) numbered at the present time from SCA1 to SCA37 according to individually discovered genes. We review naturally mutated mice with cerebellar atrophy together with induced SCA mutations. Known for a longer time, the spontaneous mutants have been more thoroughly evaluated than the induced mutants and, therefore, serve as contrast with what remains to be determined in the newer models. Among the older models, we selected the most behaviorally characterized ones and those with more selective damage to the cerebellar cortex.

The main tests of motor coordination used to test natural mutations are stationary beam, suspended wire, and rotorod tests, all sensitive to cerebellar lesions [2, 3]. Mice are placed on a stationary beam (Fig. 1a) and either walk along it or remain still. In the suspended wire test, mice are placed upside down on a horizontal wire and stay upside down with two paws or four. If able to maintain their position with four paws, they can lift themselves upright on a sidebar of a coat hanger (Fig. 1b). On the rotorod (Fig. 1c), mice are placed on a beam that rotates and must move in synchrony with it. In all three tasks, latencies before falling and number of falls are measured. In stationary beam and coat hanger tasks, movement time (MT) can be estimated as defined by the time taken to walk or slide across the beam or bar. Different types of MT have been used in the coat hanger version to delineate more precisely difficulties encountered while moving along the horizontal bar and climbing atop the diagonal bar. Since animals support their body weight in an upside down position, the suspended wire test requires muscle strength all the more, relevant in this context because one of the main features of cerebellar symptoms is hypotonia. In some lesioned animals, the loss in balance on the stationary beam can be compensated by remaining still, so that an additional measure can be used to

✉ Robert Lalonde
robert.lalonde@univ-rouen.fr

[1] Department of Psychology, University of Rouen, 76821 Mont-Saint-Aignan Cedex, France

[2] Laboratory of Stress, Immunity, and Pathogens EA7300, and CHRU of Nancy, University of Lorraine, 54500 Vandoeuvre-les-Nancy, France

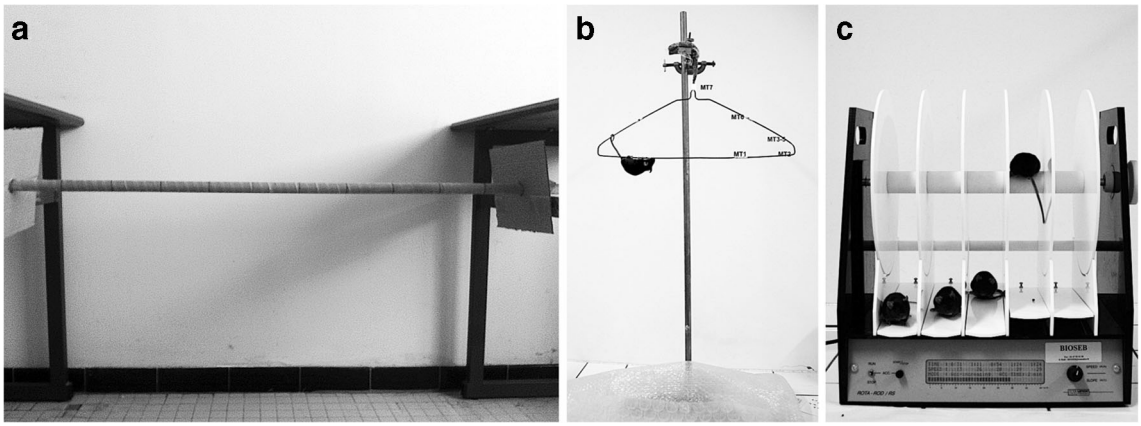

Fig. 1 **a** Stationary beam test: mice are placed on top of the beam and left there until they fall. **b** Coat hanger test: mice are placed upside down above a padded surface and movement times (MTs) are measured until the mice reach the mid-point (MT1) or the end (MT2) of the horizontal bar (nose criterion), lift themselves on the diagonal bar with two, three, or four paws (MT3–MT5) and reach up to the mid-point (MT6) or top (MT7) of the diagonal bar. **c** Rotorod test: mice are placed on top of the rotating beam and left there until they fall or turn passively

disclose the deficit, namely the distance traveled along the beam or the time taken to reach the end of the beam. In contrast, the rotorod cannot be compensated by immobility unless the animal wraps its legs around the beam. After two successive rotations of this passive type, for example, the animal should be removed and the trial ended as if it fell.

Natural Mouse Mutations with Cerebellar Atrophy

Table 1 illustrates neurobehavioral characteristics of mice with natural mutations causing relatively selective degeneration of the cerebellar cortex and deficits in motor coordination tests [2, 3].

Grid2

The semidominant *Lurcher* mutation causes a gain-in-malfunction of *Grid2* located on chromosome 6 and encoding the GluRδ2 ionotropic glutamate receptor associated with the amino-methyl-isoxazolepropionate (AMPA) receptor [10]. Grid2 mRNA is predominantly expressed in cerebellar Purkinje cells [11]. The depolarized membrane potential of the $Grid2^{Lc}$ encoded receptor is probably responsible for the nearly total loss of Purkinje cells from postnatal weeks 2 to 4 [4].

Two autosomal recessive *hot-foot* alleles (*4J* and *nancy*) cause different deletions in the coding sequences of *Grid2* [12, 13]. For the *ho-4J* allele, the truncated GluRδ2 protein is expressed in Purkinje cell soma without being transported to the cell surface [14]. The main neuropathological marker in $Grid2^{ho\text{-}nancy}$ mutants is defective parallel fiber–Purkinje cell innervation and mild depletion of cerebellar granule cells, resulting in cerebellar ataxia and a hopping gait reminiscent of mice walking on a hot plate [5]. In contrast to the gain-in-malfunction subtending the *Lc* allele, *ho* alleles are nonfunctional, as indicated by the similar phenotype seen in the *Grid2* targeted null mutation marked by reduced synaptic contacts on Purkinje cells, ataxia, and motor coordination deficits [15]. Thus, in $Grid2^{Lc}$ mutants [16–20] and $Grid2^{ho\text{-}nancy}$ mutants [5, 15, 16, 21], there is cerebellar ataxia as defined as a widespread gait and defective performances on stationary beam, coat hanger, and rotorod tests relative to nonataxic controls.

Rora

The autosomal recessive *staggerer* mutation deletes *Rora* located on chromosome 9, which encodes a retinoid-like nuclear receptor involved in neuronal differentiation and maturation highly expressed in Purkinje cells [22, 23]. As in *hot-foot*, the lost function of the $Rora^{sg}$ mutation was confirmed by observing nearly identical neuropathological and behavioral phenotypes in targeted *Rora* null mutants [24, 25]. In $Rora^{sg}$ homozygotes, Purkinje cells decline in number before postnatal day 5, and at the end of the first postnatal month, 75% of them disappear [6]. Thus, the Purkinje cell loss begins at an earlier stage than $Grid2^{Lc}$ (postnatal day 8) but is less complete [4]. Even when present, metabotropic glutamate receptor type 1 (mGluR1)-mediated signaling at cerebellar parallel fiber–Purkinje cell synapses was disrupted in $Rora^{sg}$ mutants [26]. As with *Grid2* mutants, performances on stationary beam, coat hanger, and rotorod tests were deficient in $Rora^{sg}$ mutants relative to nonataxic controls [15, 16, 27, 28].

Agtpbp

The autosomal recessive *Purkinje cell degeneration* (*pcd*) mutation affects *Agtpbp1* located on chromosome 13 and encoding ATP/GTP binding protein 1 [29]. In normal mouse brain, Agtpbp1 mRNA is prominent in Purkinje

Table 1 Neurobehavioral characteristics of natural mouse mutations with cerebellar atrophy

Mutant	Chromosome	Neuropathology	Motor test	Genetic reference
Grid2^{Lc}	6	Purkinje cell loss	↓ Stationary beam Coat hanger Rotorod	Caddy and Biscoe [4]
Grid2^{ho}	6	Granule cell loss	↓ Stationary beam Coat hanger Rotorod	Guastavino et al. [5]
Rora^{sg}	9	Purkinje cell loss	↓ Stationary beam Coat hanger Rotorod	Herrup and Mullen [6]
Agtpbp1^{pcd}	13	Purkinje cell loss	↓ Coat hanger Rotorod	Mullen et al. [7]
Reln^{rl}	5	Granule cell loss	↓ Stationary beam Coat hanger Rotorod	Mariani et al. [8]
Dab1^{scm}	5	Granule cell loss	↓ Stationary beam Coat hanger Rotorod Vertical grid	Sweet et al. [9]

↓, decreased performance

cells, mitral cells of olfactory bulb, thalamic neurons, and retinal photoreceptors, all of them prone to degeneration in the mutant. Several alleles of the affected gene have been discovered, including *1J* on C57BR/cdJ, *2J* on SM/J, and *3J* on BALB/cByJ backgrounds, respectively. The *1J* allele was subsequently transferred to B6C3-a/a and C57BL/6J backgrounds and the *2J* allele to C57BL/6J. The predominant pathology in *Agtpbp1*$^{pcd\text{-}1J}$ mutants concerns almost total Purkinje cell loss from the third to the fourth postnatal week [7, 30].

Agtpbp1$^{pcd/1J}$ mutant mice were deficient relative to nonataxic controls on coat hanger and rotorod tests [31]. When three adult mutant models were placed on the same rectangular stationary beam, only *Rora*^{sg} mutants [27] fell sooner than their nonataxic controls, not *Grid2*^{Lc} mutants [17] or *Agtpbp1*$^{pcd/1J}$ mutants [31]. This result may be explained by the almost total loss of Purkinje cells in *Grid2*^{Lc} and *Agtpbp1*$^{pcd/1J}$ mutants but a 75% loss in *Rora*^{sg}, so that the existence of dysfunctional Purkinje cells and their abnormal dendritic arborization appears to cause a worse phenotype than their absence. A second possibility is the earlier onset of Purkinje cell degeneration in *Rora*^{sg} relative to the other two worsens the behavioral phenotype in the adult.

Reln and *Dab1*

The autosomal recessive *reeler* mutation disrupts *Reln* located on chromosome 5 and encoding reelin [32, 33]. Two *Reln*^{rl} alleles have been discovered: *Jackson* (J) and *Orleans* (Orl). The *Jackson* allele on the C57BL/6 or the hybrid B6C3 background has a deletion of the entire gene and *Orleans* on the Balb/c background a 220-bp deletion in the open reading frame, causing a frame shift [34]. Reelin is an extracellular matrix protein involved in neural adhesion and migration at critical stages of development [32–35]. *Reln*$^{rl\text{-}J}$ and *Rel*^{orl} mutants display cell ectopias in the cerebellum, hippocampus, and neocortex [8, 36, 37]. In line with elevated expression of Reln mRNA in granule but not Purkinje cells [38], the former constitutes the main depleted cell type in the cerebellum of the mutant [39]. Among mutations upstream of the reelin signaling pathway, disruption of *Dab1* located on chromosome 4 and encoding disabled homolog 1 characterizes the autosomal recessive *Dab1*^{scm} (*scrambler*) mutation with a similar phenotype to *Reln*^{rl} ones [9]. Relative to nonataxic controls, the performances on stationary beam, coat hanger, and rotorod tests were deficient in *Relrl*^{orl} mutants [40] and *Dab1*^{scm} mutants [41], the latter being also deficient in climbing a vertical grid, a test better adapted to their motor capacity [42].

Genetically Modified Mouse Mutations with Cerebellar Atrophy

To provide features of SCA subtypes (Tables 2 and 3), genetically modified mice have been generated with human or animal versions of the mutated genes (transgenic) or with targeted deletion of the affected genes (null mutants).

SCA1

SCA1 is an autosomal dominant disorder caused by over 39 cytosine–adenine–guanine (CAG) trinucleotide repeats of the *ATXN1* gene located on chromosome 6 and encoding ataxin-1 [95], found in Purkinje and other cells [96]. The CAG or CAA triplet is specific for the amino acid glutamine, excessively repeated in several diseases designated as polyglutamine and including cerebellar or basal ganglia anomalies such as Huntington's disease. SCA1 causes adult-onset degeneration of cerebellar cortex and brainstem, leading to ataxia, dysarthria, and bulbar symptoms. Other SCA genes have been numbered and designated as "ataxins" (e.g., ataxin-2, ataxin-3, etc) when no previous function had yet been discovered.

To mimic human SCA1 disease, transgenic mice containing 82 CAG repeats in *ATXN1* driven by the Purkinje-cell–specific *Pcp2* promoter were generated [43]. The cerebellar molecular layer of conditional *ATXN1*/Q82 transgenic mice is thinner and Purkinje cells are ectopic and shrunken [97], probably due to a gain-in-malfunction mutation, because *Atxn1* null mutants display neither Purkinje cell pathology nor ataxia [98]. Unlike natural mutations described above whose ataxia is noticeable during the first 3 weeks of life, the ataxia seen in *ATXN1*/Q82 mice is only evident at 3 months [97]. Nevertheless, the mutants were already impaired on rotorod and stationary beam tests as early as 5 weeks of age, when cytoplasmic vacuoles in Purkinje cells are their main histopathologic feature. At 1 year of age, *ATXN1*/Q82 transgenic mice became impaired in footprint analyses. Compared to mutants with 82 CAG repeats, *ATXN1*/Q30 transgenic mice with 30 CAG repeats developed overt ataxia at a later onset and a milder form of Purkinje cell degeneration [44]. As seen in *Rora*^{sg} mutants [26], mGluR1-mediated signaling at cerebellar parallel fiber–Purkinje cell synapses was disrupted in *ATXN1*/Q82 transgenic mice [99]. Facilitated MGluR1 signaling after intracerebellar injection of the $GABA_B$ receptor agonist, baclofen, improved their rotorod performance. Contrariwise, intravermal injection of lentiviral vectors containing *ATXN1*/Q76 or *ATXN1*/Q30 with green fluorescent protein impaired rotorod performance in wild-type mice. The efficacy of intrathecally injected mesenchymal stem cells was also tested in *ATXN1*/Q82 mice [100]. The cells mitigated Purkinje cell ectopias, dendritic thinning, and rotorod deficits, prompting the possible use of this technique in other neurodegenerative conditions [101]. Likewise, the injection of neural precursor cells derived from the subventricular zone into the cerebellar white matter of *ATXN1*/Q82 mice recovered Purkinje cell loss and ectopias as well as increasing grip strength and rotorod performance [102].

Another strategy used to modify the *ATXN1*/Q82 phenotype comprises interbreeding with other mutants. Relative to the single transgenic, *ATXN1*/Q82 mice crossbred with *Trp53* null mutant mice lacking the p53 protein involved in cell death counteracted Purkinje cell heterotopias and dendritic thinning as well as molecular layer shrinkage, though without affecting rotorod performance or formation of ataxin-1 nuclear inclusions [103]. When *ATXN1*/Q82 transgenic mice were crossbred with mice overexpressing the inducible form of rat *Hsp70* encoding a molecular chaperone involved in protein folding, Purkinje cells had thicker and more arborized dendritic branches than the single transgenic but this time rotorod performance improved despite the absence of any change on ataxin-1 aggregates [104]. In contrast, *ATXN1*/Q82 transgenic mice bred with *Ube3a* null mutants lacking E6-AP ubiquitin ligase had fewer ataxin-1 aggregates, but the Purkinje cell pathology was worse than the single transgenic, so that aggregates seem to have a protective role in this case [105]. *ATXN1*/Q82 mice were also evaluated on whether RNA interference inhibits polyglutamine-induced neurodegeneration [106]. This time, midline cerebellar injection of recombinant adeno-associated virus vectors expressing short hairpin RNAs resolved ataxin-1 inclusions in Purkinje cells, restored cerebellar molecular thickness, and improved rotorod performance. From two of the models described above [104, 106], different conclusions may be reached in regard to the role of ataxin-1 aggregates on sensorimotor coordination. In one model [106], resolved ataxin-1 inclusions improved rotorod performance, leading to the conclusion that experimental therapies should aim at reducing the aggregates. But in another model [104], rotorod performance improved despite the absence of any change in ataxin-1 aggregates, leading to the conclusion that the aggregates are irrelevant in regard to function. These results underline the sensitivity of the rotorod test over a neuropathological marker as a target in evaluating experimental therapies.

An inducible tetracycline-regulated *ATXN1*/Q82 mouse model has also generated with a transgene controlled by the *Pcp2* promoter with similar characteristics, including heterotopic Purkinje cells with cytoplasmic vacuoles and nuclear inclusions as well as reduced Purkinje cell dendritic arborization and lower cerebellar mGluR1 levels combined with rotorod deficits [45]. Halting inducible *ATXN1*/Q82 expression with doxycycline in the drinking water reduced cytoplasmic vacuoles and nuclear inclusions and restored Purkinje cell dendritic arborization, cerebellar mGluR1 levels, and rotorod deficits, implicating the Purkinje cell–parallel fiber synapse on motor performance.

Table 2 Neurobehavioral characteristics of SCA1 to SCA8 mouse mutations with cerebellar atrophy on sensorimotor tests

Mutant	Promoter	Neuropathology	Motor test	Identifier reference
ATXN1/Q82	*Pcp2*	Purkinje cell loss	↓ Stationary beam Rotorod	SCA1 Burright et al. [43]
ATXN1/Q30	*Pcp2*	Purkinje cell loss	?	SCA1 Fernandez-Funez et al. [44]
Inducible *ATXN1*/Q82	*Pcp2*	Ectopic Purkinje cells	↓ Rotorod	SCA1 Zu et al. [45]
Atxn1/Q154	Endogenous	Purkinje cell loss	↓ Rotorod	SCA1 Watase et al. [46]
Atxn1/Q78	Endogenous	No atrophy	↓ Rotorod	SCA1 Lorenzetti et al. [47]
ATXN2/Q58	*Pcp2*	Purkinje cell loss	↓ Stationary beam Rotorod	SCA2 Huynh et al. [48]
ATXN2/Q75	*ATXN2*	Purkinje soma shrinkage	↓ Rotorod	SCA2 Aguiar et al. [49]
ATXN2/Q127	*Pcp2*	Purkinje cell loss	↓ Rotorod	SCA2 Hansen et al. [50]
ATXN2/Q72-BAC	*ATXN2*	Reduced Purkinje cell dendrite branches	↓ Rotorod	SCA2 Dansithong et al. [51]
Atxn2/Q42	*Atxn2*	Ataxin-2 aggregates	↓ Rotorod	SCA2 Damrath et al. [52]
ATXN3/Q69	*Pcp2*	Purkinje cell ectopias, thin dendrite branches	↓ Rotorod	SCA3 Torashima et al. [53]
ATXN3/Q71	*Prp*	Nuclear inclusions	↓ Rotorod	SCA3 Goti et al. [54]
ATXN3/Q79-*Pcp2*	*Pcp2*	Purkinje cell loss	?	SCA3 Ikeda et al. [55]
ATXN3/Q79-*Prp*	*Prp*	Nuclear inclusions	↓ Rotorod	SCA3 Chou et al. [56]
ATXN3/Q94	*CMV*	Shrunken cells	↓ Rotorod	SCA3 Silva-Fernandes et al. [57]
ATXN3/Q135	*CMV*	Loss in dentate volume and pontine cell number	↓ Stationary beam Wire suspension Rotorod	SCA3 Silva-Fernandes et al. [58]
ATXN3/Q148-*Prp*	*Prp*	Nuclear inclusions	?	SCA3 Bichelmeier et al. [59]
ATXN3/Q148-*Hd*	*Hd*	Nuclear inclusions	↓ Rotorod	SCA3 Boy et al. [60]
Atxn3/Q82	Endogenous	Nuclear inclusions	NE Stationary beam Rotorod	SCA3 Chou et al. [61]
ATXN3/Q91	Endogenous	Purkinje cell loss	↓ Rotorod	SCA3 Switonski et al. [62]
Inducible *ATXN3*/Q77	*Prp*	Shrunken Purkinje cells, thin molecular layer	↓ Rotorod	SCA3 Boy et al. [63]
ATXN3/YAC-Q84	Endogenous	Cell loss in pons and dentate	↓ Stationary beam	SCA3 Cemal et al. [64]

Table 2 (continued)

Mutant	Promoter	Neuropathology	Motor test	Identifier reference
ATXN3/YAC-Q67	Endogenous	Cell loss in pons and dentate	?	SCA3 Cemal et al. [64]
Sptbn2 KO	Not applicable	Purkinje cell loss	NE Wire suspension ↓ Stationary beam Rotorod	SCA5 Perkins et al. [65]
Sptbn2 KO	Not applicable	Thin molecular layer, shrunken Purkinje cells	↓ Wire suspension Rotorod	SCA5 Stankewich et al. [66]
Inducible *SPTBN2* deletion	*CMV*	Thin molecular layer	↓ Rotorod	SCA5 Armbrust et al. [67]
CACNA1A/Q27	*CMV* and *ACTB*	Purkinje cell loss	↓ Stationary beam Inclined screen Rotorod	SCA6 Mark et al. [68]
CACNA1A/CT-short	*CMV* and *ACTB*	Purkinje cell loss	↓ Rotorod NE stationary beam	SCA6 Mark et al. [68]
CACNA1A/Q33	*Pcp2*	Thin molecular layer	?	SCA6 Du et al. [69]
Cacna1a/Q84	Endogenous	Purkinje cell loss	↓ Stationary beam Rotorod	SCA6 Watase et al. [70]
Cacna1a/Q118	Endogenous	Purkinje cell loss	↓ Rotorod	SCA6 Unno et al. [71]
CACNA1A/Q33	*Pcp2*	Thin molecular layer	?	SCA6 Du et al. [72]
ATXN7/Q52	PDGF	Shrunken Purkinje soma, smaller dendritic branches	↓ Rotorod	SCA7 Chou et al. [73]
ATXN7/Q92-*Pcp2*	*Pcp2*	Reduced Purkinje cell dendrite branches	↓ Rotorod	SCA7 Yvert et al. [74]
ATXN7/Q92- *Gfa2*	*Gfa2*	Purkinje cell misalignment and dendrite thinning	↓ Rotorod	SCA7 Custer et al. [75]
ATXN7/Q92-*Prp*	*Prp*	Purkinje cell loss	↓ Rotorod	SCA7 Garden et al. [76]
ATXN7/Q10 *ATXN7*/Q128	*PDGF*	Ataxin-7 aggregates	?	SCA7 Yvert et al. [77]
ATXN7/BAC-Q92	*Prp*	Purkinje cell loss	↓ Rotorod	SCA7 Furrer et al. [78]
Atxn7/Q266	Endogenous	Shrunken Purkinje soma	↓ Rotorod	SCA7 Yoo et al. [79]
ATXN7/Q100 lentivirus	*PGK1*	Ataxin-7 aggregates	↓ Rotorod	SCA7 Alves et al. [80]
Atxn8 KO	Not applicable	Thin molecular layer	↓ Rotorod	SCA8 He et al. [81]
ATXN8/Q116	Endogenous	Nuclear aggregates	↓ Rotorod	SCA8 Moseley et al. [82]

↓, decreased performance; *NE*, no effect; *?*, no sensorimotor test was evaluated

Table 3 Neurobehavioral characteristics of SCA10 to SCA28 mouse mutations with cerebellar atrophy on sensorimotor tests

Mutant	Promoter	Neuropathology	Motor test	Identifier reference
ATNX10 KO	Not applicable	Pontine nuclei loss	?	SCA10 White et al. [83]
Kcnc3 KO	Not applicable	?	↓ Stationary beam	SCA13 McMahon et al. [84]
PRKCG/H101Y	*CMV*	Purkinje cell loss	?	SCA14 Zhang et al. [85]
Inducible *PRKCG*/S119P	*Pcp2*	Climbing fiber poly-innervation of Purkinje cells	↓ Rotorod	SCA14 Shuvaev et al. [86]
Itpr1 KO	Not applicable	?	?	SCA15 van de Leemput et al. [87]
Itpr1 KO	Not applicable	?	?	SCA15 Matsumoto et al. [88]
opt	Not applicable	Abnormal calcium responses in Purkinje cells	?	SCA15 Street et al. [89]
TBP/Q109	*Pcp2*	Purkinje cell loss	↓ Rotorod	SCA17 Chang et al. [90]
Inducible *TBP*/Q105	Endogenous	Purkinje cell loss	↓ Stationary beam Rotorod	SCA17 Huang et al. [91]
TBP/Q64	*Prp*	Purkinje cell loss	↓ Stationary beam NE rotorod	SCA17 Kelp et al. [92]
Fgf14	Not applicable	Parallel fiber anomalies	↓ Inclined screen Inverted screen Rotorod	SCA27 Wang et al. [93]
Afg3l2	Not applicable	Granule and Purkinje cell loss	↓ Inclined grid Stationary beam Rotorod	SCA28 Maltecca et al. [94]

↓, decreased performance; *NE*, no effect; *?*, no sensorimotor test was evaluated

Other SCA1 models overexpress mouse not human gene mutations. In particular, *Atxn1*/Q154 knockin mice bear 154 CAG repeats of the mouse *Atxn1* locus and express full-length mutant ataxin-1 in its endogenous expression pattern and context, causing a loss in Purkinje cell number and dendritic branching, ataxia, paw clasping, and rotorod deficits before the onset of ataxia [46]. In contrast, *Atxn1*/Q78 knockins had no obvious sign of cerebellar atrophy or ataxia but were still deficient on the rotorod [47]. To establish the role of the mutation, a cerebellar extract was injected from *Atxn1*/Q154 knockin or wild-type mice into deep cerebellar nuclei of *Atxn1*/Q78-Q2 knockins [107]. The cerebellar extract from *Atxn1*/Q154 knockins increased oligomer formation in cerebellum and brainstem of *Atxn1*/Q78 knockins. As a form of experimental therapy, intraperitoneal injection of *Atxn1*/Q154 knockin mice with the anti-oligomer antibody, F11G3, reduced oligomers in Purkinje cells and improved rotorod acquisition. In addition, *Atxn1*/Q154 crossed with a *VEGFA* transgenic line expressing human vascular endothelial growth factor-A increased calbindin staining intensity of Purkinje cells and molecular layer thickness as well as speeding up rotorod acquisition [108]. Moreover, *Atxn1*/Q154 knockins acquired the rotorod task more quickly after a lithium diet [109], a manipulation affecting the neurochemistry of the cerebellum at the level of energy metabolism, purines, and unsaturated free fatty acids as well as aromatic- and sulfur-containing amino acids [110]. Mitochondria-targeted antioxidant MitoQ also ameliorated motor coordination in *Atxn1*/Q154 knockins [111].

Proteins interacting with ataxin-1 can promote SCA1-related neurodegeneration. In particular, pumilio1 regulates ataxin-1 levels in cells [112]. *Pum1* null mutant mice lacking pumilio1 had higher ataxin-1 levels in the cerebellum and cerebrum than wild type, leading to loss of Purkinje cell number and dendritic arborization. This form of neuropathology likely contributes to delayed acquisition of the rotorod task,

the presence of hind-paw clasping, more horizontal but less vertical activity in the open field, and footprint anomalies such as a wider stance, shorter stride length, and greater stride frequencies. *Pum1* null mutants crossed with *Atxn1*/Q154 knockins increased the severity of the loss in Purkinje cell number and dendritic arborization and caused earlier onset of hind-paw clasping and mortality than the single transgenic. Contrariwise, Purkinje cell loss and dendritic arborization as well as rotorod deficits and paw clasping in *Pum1* null mutants were mitigated when intercrossed with *ATXN1* null mutants.

We notice from these series of experiments that the rotorod test is the standard most often used to phenotype SCA1 models and assess the possible improvement in motor functions following various forms of experimental therapy, the stationary beam test being used only once [97]. It remains to be determined to what extent the wire suspension test may contribute to phenotype more precisely SCA1 models.

SCA2

Like SCA1, SCA2 is an autosomal dominant disorder with CAG repeat expansions causing a gain-in-malfunction and leading to Purkinje cell degeneration, limb incoordination, and dysarthria [113, 114]. Disease occurs whenever CAG repeats rise above 31 in *ATXN2* located on chromosome 12 and encoding ataxin-2. As with the *Atxn1* knockout (KO), the *Atxn2* mouse KO shows no sign of ataxia, prompting the conclusion that the disease leads to a gain-in-malfunction [115].

ATXN2/Q58 mice contain 58 CAG repeats of the transgene driven by the *Pcp2* promoter, leading to Purkinje cell loss, paw clasping, reduced stride length, and rotorod deficits [48]. The mutants also had longer MTs and more foot-slips than wild type on the stationary beam [116]. In experimental therapies, *ATXN2*/Q58 transgenic mice fed dantrolene, a stabilizer of intracellular calcium signaling, exhibited a lesser degree of Purkinje cell loss as well as faster MTs and fewer foot-slips on the stationary beam. Moreover, adenovirus-mediated expression of inositol 1,4,5-phosphatase into deep cerebellar nuclei alleviated electrophysiological anomalies in Purkinje cells as well as accelerating MTs and reducing foot-slips on the stationary beam and increasing latencies before falling from the rotorod [117]. These results indicate that inhibiting enzyme-mediated calcium signals may provide therapeutic benefits in patients. Purkinje cell loss and rotorod impairment were also alleviated after intraventricular transplantation of human mesenchymal stem cells [118].

A second SCA2 transgenic murine model expresses the full-length human *ATXN2* gene with 75 CAG repeats controlled by the self *Atxn2* promoter [49]. *ATXN2*/Q75 transgenic mouse brains contain Purkinje cell body shrinkage and loss of dendritic arborization and the mice have rotorod deficits. A third transgenic model with a longer expansion, *ATXN2*/Q127, was generated under control of the *Pcp2* promoter [50]. *ATXN2*/Q127 mutants have cytoplasmic ataxin-2-containing insoluble aggregates in Purkinje cells, Purkinje cell loss, thinning of the cerebellar molecular layer, and rotorod deficits.

A fourth model, the *ATXN2*/Q72-BAC transgenic mouse, was generated with 72 CAG repeats of the human *ATXN2* gene controlled by the endogenous promoter on bacterial artificial chromosomes (BAC) [51]. *ATXN2*/Q72-BAC transgenic mice had smaller dendritic arborization and rotorod deficits. A knockin model of SCA2 disease was generated by homologous recombination of embryonic stem cells to replace the endogenous *Atxn2* gene with a mutagenized mouse version containing 42 CAG repeats driven by the *Atxn2* promoter [52]. *Atxn2*/Q42 knockins had cytoplasmic ataxin-2-containing aggregates and rotorod deficits, though without displaying overt ataxia or any change in footprint analyses, grip strength, or open-field activity. Thus, the rotorod deficit seen in *Atxn2*/Q42 knockins precedes overt ataxia, as reported in *ATXN1*/Q82 mice [97] described above. And so the rotorod and perhaps other motor tests may be used in experimental therapies of SCA2 mutants before dysfunction appears under the naked eye.

SCA3

Like SCA1 and SCA2, SCA3, also called Machado–Joseph disease, is due to a polyglutamine expansion, this time an expansion of over 45 CAG repeats in *ATXN3* located on chromosome 14 and encoding ataxin-3 [119–121]. SCA3 causes prominent cerebellar signs such as gait ataxia, dysmetria, and dysarthria, along with parkinsonian signs [122] resulting from lesions in the cerebellum, pontine nuclei, and substantia nigra pars compacta [123]. Ataxin-3 binds to the type 1 inositol 1,4,5-trisphosphate receptor, the intracellular calcium release channel [124].

Several SCA3 mouse models are available [125], one of which featuring *ATXN3*/Q69 transgenic mice expressing the mutant gene driven by the *Pcp2* promoter [53]. *ATXN3*/Q69 mice showed Purkinje cell ectopias and thinner dendrite branching along with overt ataxia and delayed rotorod acquisition, probably due to a gain-in-malfunction mutation, because *Atxn3* null mutants display neither Purkinje cell pathology nor ataxia [126]. Purkinje cell ectopias and rotorod performance ameliorated in *ATXN3*/Q69 mice after midline cerebellar injection of lentiviral vectors expressing wild-type *CRMP1* (collapsin response mediator protein, CRAG), which degrades polyglutamine proteins via the ubiquitin–proteasome pathway [53]. In addition, integrase-defective lentiviral vectors injected into the cerebellum decreased ataxin-3 aggregates and improved rotorod performance [127]. Moreover, *ATXN3*/Q69 mice had fewer nuclear

inclusions and higher cerebellar calbindin immunoreactivity along with thicker molecular and granular layers as well as higher latencies before falling off the rotorod, larger stride length in footprint analyses, and higher horizontal activity in the open field after intracerebellar injection of lentiviral vectors of short-hairpin RNAs encoding allele-specific silencing sequences [128].

A second SCA3 model employs the *ATXN3*/Q71 transgene driven by the murine *Prp* promoter, exhibiting ataxin-3 nuclear inclusions and substantia nigra pars compacta cell loss combined with ataxia, tremors, seizures, footprint anomalies, grip strength weakness, open-field hypoactivity, and rotorod deficits [54]. A third SCA3 transgenic model, *ATXN3*/Q79-*Pcp2*, expresses truncated ataxin-3 with an expanded polyglutamine stretch driven by the *Pcp2* promoter [55]. *ATXN3*/Q79-*Pcp2* mice have Purkinje cell loss and overt ataxia. A fourth model with the same number of repeats, *ATXN3*/Q79-*Prp*, was generated with a transgene driven by the murine *Prp* promoter [56]. *ATXN3*/Q79-*Prp* transgenic mice display mutated ataxin-3 nuclear inclusions in dentate, pontine, and nigral nuclei; an ataxic gait; forelimb clasping; open-field hypoactivity; and rotorod deficits. The fact that mutated ataxin-3 directly causes cell death is shown by findings in cultured cerebellar and nigral neurons [129]. In these *ATXN3*/Q79-*Prp* transgenic mice, intraperitoneal injection of H1152, an inhibitor of rho-kinase (ROCK), decreased ataxin-3 protein concentrations at the cerebellar, pontine, and neocortical sites as well as pontine cell death while counteracting open-field hypoactivity and rotorod deficits [130]. Likewise, footprint analyses of gait, open-field hypoactivity, and rotorod deficits improved after intraperitoneal injection of sodium butyrate, an inhibitor of histone deacetylase, an effect that reverses transcriptional downregulation [131]. Moreover, pontine nuclei degeneration and rotorod deficits were mitigated after oral administration of an adenosine A2A receptor agonist, T1-11 [N6-(4-hydroxybenzyl) adenosine], extracted from *Gastordia elata*, a Chinese medicinal herb, or its synthetic analog, JMF1907 [N6-(3-indolylethyl) adenosine] [132].

An *ATXN3* transgene with a longer Q94 expansion driven by the *CMV* promoter exhibited mutant ataxin-3 inclusions and shrunken cells in the cerebellum, pons, and substantia nigra combined with open-field hypoactivity and deficits on rotorod but not vertical pole or footprint assays [57]. Thus, the *ATXN3*/Q94 transgenic resembles the *Atxn2*/Q42 knockin [52] and *ATXN1*/Q82 transgenic [97] which display rotorod deficits with no overt ataxia or anomalies in footprint analyses.

Polyglutamine repeats were further expanded with the *ATXN3*/Q135 transgene also regulated by the *CMV* promoter [58]. *ATXN3*/Q135 mutants have ataxin-3 nuclear inclusions and lower dentate nucleus volume and pontine nucleus number, as well as substantia nigra gliosis, causing ataxia, hindlimb clasping, tremor, shorter stride length, weaker grip strength, higher latencies before traversing the stationary beam, and lower latencies before falling off the hanging wire or rotorod. Pontine cell number and ataxin-3 nuclear inclusions as well as stationary beam and rotorod performance improved after intraperitoneal injections of 17-DMAG, inhibitor of Hsp90, a heat shock protein.

Unlike wild-type mice where ataxin-3 is present in the cytoplasm, *ATXN3*/Q70 and *ATXN3*/Q148-*Prp* transgenes controlled by the murine *Prp* promoter result in brain tissue containing ubiquitin- and ataxin-3-positive nuclear inclusions [59, 133]. The *ATXN3*/Q70 model showed shrunken Purkinje cell bodies and limb-clasping; both models displayed overt ataxia and tremor [59]. A similar *ATXN3*/Q148-*Hd* transgene driven by the rat *Hd* promoter was generated, exhibiting ataxin-3-positive nuclear inclusions in Purkinje and pontine cells along with rotorod deficits [60]. They also showed home-cage hyperactivity at a young age but yet home-cage hypoactivity at an older age.

Atxn3/Q82 knockin mice were generated by introducing the murine gene with 82 polyglutamine repeats at the mouse locus, accumulating mutant ataxin-3 nuclear inclusions in Purkinje cells, pons, and substantia nigra [61]. However, 1-year-old knockin mice did not differ from wild type on stationary beam, rotorod, or open-field tests. In contrast, *ATXN3*/Q91 knockin mice generated by introducing the human gene with 91 polyglutamine repeats at the mouse locus exhibited astrogliosis in the cerebellum and susbstantia nigra, Purkinje cell loss, and rotorod deficits [62].

Inducible double *ATXN3*/Q77 transgenic mice were generated by applying the tetracycline-off system under control of the hamster *Prp* promoter, causing nuclear inclusions, a thinner molecular layer and smaller Purkinje cells, home-cage hyperactivity, limb-clasping, smaller steps in footprint analyses, and rotorod deficits [63]. The prion protein promoter drives the expression of a fusion protein tTA (tetracycline transactivator) consisting of the tetracycline repressor (TetR) and a transcription activation domain (AD) in the promoter construct. In the absence of tetracycline, the tTA protein can bind to the tetracycline responsive element (TRE) of a *CMV* minimal promoter in the responder construct, which activates *ATXN3* transcription. When tetracycline (Tc) or one of its derivatives such as doxycycline binds to tTA and abolishes the binding of tTA to the responder construct, *ATXN3* transcription is blocked. Crossbreeding the *PrP* promoter line with *ATXN3* responder mouse lines yielded double transgenic mice. In responder line 2904 with 77 CAG repeats, nuclear aggregates staining positive for ataxin-3 formed along with a thinner molecular layer and smaller Purkinje cells. The rotorod deficits were reversed by doxycycline. To improve behavior with a *N*-methyl-D-aspartate (NMDA) glutamate receptor antagonist in *ATXN3*/Q77 mice, riluzole was dissolved in drinking water, which reduced soluble ataxin-3 levels but also calbindin expression in Purkinje cells and increased

ataxin-3-positive accumulations without affecting home-cage hyperactivity and even worsened rotorod performance [134].

Three more SCA3-related models exist, this time with yeast artificial chromosomes (YACs), namely *ATXN3*/YAC-Q84, *ATXN3*/YAC-Q67, and *ATXN3*/YAC-Q15 transgenes under control of endogenous elements [64]. Unlike the expanded (CAG)84 allele, the expanded (CAG)76 allele contracted to 64, 67, and 72 repeats in the original 76 repeats. *ATXN3*/YAC-Q84 and *ATXN3*/YAC-Q67, but not *ATXN3*/YAC-Q15 transgenic mice, exhibited cell loss in pons and dentate nuclei with a widespread gait, fore and hind-limb clasping, and tremor. A second report in *ATXN3*/YAC-Q84 transgenics revealed fewer than normal neuronal counts in pontine and substantia nigra, higher MTs and foot-slips on the stationary beam, and shorter stride length on footprint patterns [124]. *ATXN3*/YAC-Q84 transgenic mice fed dantrolene had faster MTs and fewer foot-slips on the stationary beam and elevated stride length on footprint patterns. Moreover, *ATXN3*/YAC-Q84 mice had restored Purkinje cell firing and faster MTs on the stationary beam after intraperitoneal injection of an activator of potassium channels, SKA-31 [135]. Likewise, ataxin-3 nuclear accumulation was mitigated in *ATXN3*/YAC-Q84 mice by artificial microRNA mimics targeting the 3′-untranslated region of *ATXN3* [136].

That mutant *ATXN3* can directly affect normal mice is indicated by findings that injected lentiviral vectors encoding full-length human mutant *ATXN3* into the mouse cerebellum of C57/BL6 mice cause intranuclear inclusions, neuropathological abnormalities, and neuronal death along with motor coordination deficits, a wide-based gait, and hyperactivity [137]. As in the SCA1 model described above [97], decreased ataxin-3 aggregates or concentrations occurred in conjunction with improved rotorod performance in four experimental therapies of three SCA3 models [58, 127, 128, 130]. The reverse pattern was found in another model, when more ataxin-3 aggregates led to poorer rotorod performance [134]. Thus, ataxin-3 aggregates appear relevant in the context of improving motor functions in SCA3 models.

SCA5

SCA5 consists in autosomal dominant in-frame deletions and missense mutations in *SPTBN2* located on chromosome 11 and encoding beta-III spectrin, involved in membrane protein adhesion in the cytoplasm, a gene highly expressed in Purkinje cells [138–140]. The mutation-linked cerebellar cortical atrophy causes ataxia and dysarthria. SCA5 appears to result from a loss-of-function mutation in view of the ataxia of targeted null mutations of *Sptbn2*. One *Sptbn2* KO murine model exhibited Purkinje cell loss accompanied by wider hind-limb gait, tremor, increased foot-slips on the stationary beam, and decreased latencies before falling off the rotorod, though not off the suspended wire, the latter test being more dependent on muscle strength [65]. A second *Sptbn2* KO model exhibited a thinner than normal cerebellar molecular layer, shrunken Purkinje cells, ataxia, and myoclonic seizures as well as wire suspension and rotorod deficits [66].

Tet-response element (TRE) and *CMV* promoter were cloned with *SPTBN2* cDNA and the resulting mutants bred to tetracycline transactivator (tTA)/*Pcp2* transgenic mice to generate conditional bigenics expressing recombinant transgenes specifically in Purkinje cells [67]. Conditional and inducible *SPTBN2*/double transgenics with a deletion mutation are characterized by a thinner molecular layer of the cerebellar cortex, overt ataxia, and rotorod deficits. The mutants also exhibited reduced mGluR1-alpha localization at Purkinje cell dendritic spines and decreased mGluR1-mediated responses, an indication that beta-III spectrin stabilizes mGluR1 at the cell membrane.

SCA6

SCA6 is another CAG expansion disease, this time caused by mutations of *CACN1A* located on chromosome 19 and encoding the P/Q-type voltage-gated alpha-1A subunit of a calcium channel [141, 142], causing a cerebellar syndrome marked by postural ataxia as well as limb and ocular dysmetria [142]. Exon 47 undergoes alternative splicing, leading to C-terminal isoforms containing either exon 47 alone or with polyglutamine repeats [143]. Human C-terminal fragments ending at exon 46 (CT-short) or exon 47 (CT-long) ending with 27 polyglutamine residues were expressed in transgenic mice with *CMV* and *ACTB* promoters [68]. Both models had Purkinje cell loss, but onset was more precocious in *CACNA1A*/Q27 mice than *CACNA1A*/CT-short mice. *CACNA1A*/Q27 mice were deficient on stationary beam, inclined screen, and rotorod tests, whereas *CACNA1A*/CT-short mice were deficient only on the rotorod. Thus, the use of multiple tests helps delineate a more precise phenotype for two mutants of the same gene.

The C terminus of the alpha-1A subunit (alpha-1ACT) is a transcription factor that enhances expression of several Purkinje cell-expressed genes and partially rescued the phenotype of *Cacna1a* null mutants, whose electrophysiological properties resembled *leaner* and *tottering* spontaneous *Cacna1a* mutants [69]. The alpha1-ACT fragment was expressed via the *Pcp2* promoter and Tet-off system yielding *Pcp2*-tTA/TRE-alpha1-ACT mutants bred with *CACNA1A*/Q33 mice expressing 33 CAG repeats to generate double transgenic mice. *CACNA1A*/Q33 mutants have molecular layer thinning in cerebellum and gait disturbances.

Cacna1a/Q84 knockin mice were generated by introducing the mouse gene with 84 polyglutamine repeats at the mouse locus, causing cytoplasmic inclusions in Purkinje cells and rotorod deficits [70]. *Cacna1a*/Q84 knockins also displayed Purkinje cell axon anomalies in the form of torpedoes as found

in SCA6 patients [144]. *Cacna1a*/Q84 knockin mice exhibited late-onset loss of Purkinje cell number but early-onset increase in foot-slips on the stationary beam and decreased latencies before falling off the rotorod despite the absence of any change in stride length or stance width [145]. As described in some SCA1, SCA2, and SCA3 mutants, *Cacna1a*/Q84 knockins displayed rotorod deficits prior to changes in footprints. Moreover, the same pattern was found for the first time with the stationary beam. Anomalies in Purkinje cell firing rate were discernable as early as the second postnatal week [71]. A model with longer repeats, *Cacna1a*/Q118 knockin mice, exhibited cytoplasmic inclusions in Purkinje cells, reduced Purkinje cell number and dendritic branching, short-stepped walking, and rotorod deficits, all of which being absent in a knockin with fewer repeats: *Cacna1a*/Q11 [72].

SCA7

Like SCA types 1, 2, and 3, SCA7 is an autosomal dominant disorder caused by CAG trinucleotide repeats, this time concerning *ATXN7* located on chromosome 3 and encoding ataxin-7 [146–149]. Despite widespread distribution of ataxin-7, neurodegeneration mainly occurs in the cerebellum, inferior olive, pons, and retinal photoreceptors. In one large cohort of patients, glutamine repeats ranged between 37 and 130, causing ataxia, dysmetria, dysarthria, blindness, and ophthalmoplegia as the principal clinical signs [147]. CAG repeat size was inversely correlated with disease onset, determining 71% of its variability. In patients with equivalent disease durations, CAG repeats were longer in those with blindness, ophthalmoplegia, and extensor plantar reflexes. Ataxin-7 neurodegeneration appears to involve the two main protein degradation pathways in mammalian cells: the ubiquitin–proteasome system and autophagy [150].

The *ATXN7*/Q52 transgene driven by the *PDGFB* (platelet-derived growth factor beta-chain) promoter was generated in mice [73]. *ATXN7*/Q52 mice displayed shrunken Purkinje cells with ataxin-7 nuclear inclusions and reduced dendritic arborization combined with overt ataxia, hind-paw clasping, open-field hypoactivity, and rotorod deficits.

Two longer CAG expansions have been generated: *ATXN7*/Q92 transgenes expressed under control of either hamster *Pcp2* or human *RHO* (rhodopsin) promoters to affect either Purkinje cells or photoreceptors but accumulating ataxin-7 immunoreactive aggregates in each respective cell type [74]. *ATXN7*/Q92-*Pcp2* transgenic mice exhibited reduced Purkinje dendrite arborization without ectopias and rotorod deficits without overt ataxia. Another transgenic line expresses the same number of repeats but only in Bergmann glia of the cerebellum via the *Gfa2* promoter [75]. *ATXN7*/Q92-*Gfa2* mice developed Purkinje cell misalignment and dendrite thinning, ataxia, paw clasping, and rotorod deficits, implicating glial dysfunction in polyglutamine-mediated ataxia. Another murine model with 92 CAG repeats, this time driven by the *Prp* promoter was generated, *ATXN7*/Q92-*Prp*, expressing polyglutamine-expanded ataxin-7 throughout the CNS except in Purkinje cells [76]. Nevertheless, *ATXN7*/Q92-*Prp* developed shrunken Purkinje cells with diminished dendritic branches and rotorod deficits, indicating noncell autonomous cell degeneration in SCA7 pathogenesis. The accumulation of ataxin-7 immunoreactive neurons was observed in two other lines expressing 10 or 128 CAG repeats (*ATXN7*/Q10 or *ATXN7*/Q128) generated with the *PDGFB* promoter, the latter line exhibiting ataxia [77].

There also exists an *ATXN7*/BAC-Q92 murine model spatially and temporally regulated with cDNA flanked by loxP sites at the start site of translation in murine *PrP* of a bacterial artificial chromosome [78, 151, 152]. *ATXN7*/BAC-Q92 mice displayed Purkinje cell loss, molecular layer thinning, paw clasping, and rotorod deficits [78, 151]. The rotorod deficits were reversed by polyglutamine ataxin-7 excision when the single transgenic was transformed into a triple transgenic carrying additional *Pcp2*-Cre and *Gfa2*-Cre transgenes [78]. Polyglutamine ataxin-7 excision and reversal of rotorod deficits also occurred after interbreeding *ATXN7*/BAC-Q92 mice with those expressing tamoxifen-inducible Cre recombinase and administered per os tamoxifen after the onset of motor abnormalities and neuropathology [152]. In addition, cerebellar nuclei injection of recombinant adeno-associated virus vectors expressing interfering RNAs reduced nuclear inclusions in the cerebellum, thickened the cerebellar molecular layer, improved rotorod performance, and mitigated paw-clasping responses in *ATXN7*/BAC-Q92 mutants [151].

Atxn7/Q266 knockin mice contain 266 CAG repeats into the murine *Atxn7* locus with homologous recombination of embryonic stem cells. The resulting mice showed Purkinje cell shrinkage and ataxin-7 aggregates and photoreceptor degeneration combined with ataxia, tremors, myoclonic seizures, and rotorod deficits [79]. Purkinje cell shrinkage, low expression of cerebellar glutamate transporters, and rotorod deficits in *Atxn7*/Q266 knockin mice were attenuated after intercrossing with mice expressing *HGF*, that encodes hepatocyte growth factor driven by the *NSE* (neuron-specific enolase) promoter, the growth factor being normally expressed in Purkinje and granule cells [153]. Moreover, *Atxn7*/Q266 knockin mice improved after intraperitoneal injection of interferon-beta regarding ataxin-7 nuclear inclusions as well as stationary beam and horizontal ladder tests [154]. Thus, two sensorimotor tests were sensitive to a treatment in conjunction with mitigation of nuclear inclusions in a SCA7 model, as shown for the rotorod in SCA1 and SCA3 models.

In a viral-mediated model, lentiviral vectors express *ATXN7* fragments in the mouse vermis [80]. Two months after injection, mutant *ATXN7*/Q100 but not wild-type *ATXN7*

driven by the *PGK1* (phosphoglycerate kinase-1) promoter caused nuclear ataxin-7 aggregates in the cerebellum, shrinkage of granule and molecular layers near the injection site, open-field hypoactivity, missteps on the horizontal ladder, and rotorod deficits reminiscent of the transgene approach.

SCA8

Unlike the polyglutamine-related SCAs described above, SCA8 pathogenesis involves a polyleucine CTG expansion in *ATXN8* located on chromosome 13 and encoding ataxin-8 [155]. SCA8 results in ataxia, dysmetria, and nystagmus [156, 157].

Although several lines of evidence implicate a gain-in-malfunction [158], *Atxn8* null mutants limited to Purkinje cells exhibited a thinner cerebellar molecular layer and rotorod deficits [81]. The authors hypothesize that the human disease leads to a gain-in-malfunction in some areas but a lost in function of *ATXN8* in Purkinje cells. Another SCA8 mouse model was generated in which full-length human *ATXN8* with 116 CAG repeats was transcribed via its endogenous promoter. *ATXN8*/Q116 transgenic mice developed nuclear inclusions in Purkinje and basal pontine neurons, a loss in cerebellar molecular layer inhibition, and rotorod deficits [82].

SCA10

SCA10 pathogenesis is caused by autosomal dominant transmission of an intronic ATTCT pentanucleide repeat in *ATNX10* located on chromosome 22 and encoding ataxin-10 [159, 160]. The gain-in-malfunction leads to ataxia, intention tremor, dysmetria, dysarthria, nystagmus, and seizures [161–163].

McFarland and Ashizawa [164] reviewed the two existing mouse models of SCA10 (Table 3). A model containing the *ATNX10* transgene with 500 ATTCT repeats driven by the rat *Eno2* (neuronal enolase) promoter suffered from reproductive unfitness [165]. A second transgenic model containing the *ATNX10* transgene with 500 ATTCT repeats driven by the rat *Prp* promoter was fit for reproduction and showed pontine (though no cerebellar) neuropathology, ataxia, hind-limb clasping, seizures, open-field hypoactivity, and shorter steps as well as greater variability in step width on footprint analyses but normal rotorod testing [83]. This constitutes the reverse pattern of SCA1, SCA2, SC3, SCA6, and SCA7 models when anomalies of rotorod testing occurred in nonataxic mice. It would be most useful to test this SCA10 model in other sensorimotor tests to gauge the sensitivity of these tests relative to the rotorod, often appearing as the standard in cerebellar models.

SCA13

SCA13 is caused by dominant-negative missense mutations in *KCNC3* located on chromosome 19 and encoding Kv3.3, a potassium voltage-gated channel of the Kv3 subfamily [166]. SCA13 may be of childhood- or adult-onset characterized by ataxia, dysarthria, and seizures [167]. The F363L mutation in *Kcnc3* of zebrafish, corresponding to human infant-onset F448L, caused axonal path-finding errors in primary motor neurons [168]. Lentiviral expression of *Kcnc3* harboring the R424H missense mutation slowed down dendritic development and caused death of murine cultured Purkinje cells [169].

Null mutant mice lacking *Kcnc3* had increased lateral deviation and foot-slips on the stationary beam [84, 170, 171]. The motor deficits were mitigated after selective restoration of Kv3.3 channels in Purkinje cells [171].

SCA14

SCA14 is caused by autosomal dominant-negative missense mutations in *PRKCG* located on chromosome 19 and encoding the gamma isoform of protein kinase C (PKC-gamma) [172, 173]. SCA14 is characterized by cerebellar ataxia, dysarthria, and nystagmus [174].

The *PRKCG* transgene with the dominant-negative H101Y mutation driven by the *CMV* promoter yields mice with lower cerebellar PKC activity and Purkinje cell loss, a possible cause of their paw-clasping responses [85]. In another model, viral vectors containing the *PRKCG*-Green fluorescent protein transgene with the dominant-negative S119P mutation were injected into developing cerebellum, forming mutant aggregates in Purkinje cells and climbing fiber poly-innervation of Purkinje cells [86]. The first vector expresses tetracycline (tet) transactivator (tTA) under control of the *Pcp2* promoter. The second set of vectors express respective genes driven by a tet-responsive promoter transactivated by tTA. Because mutant PKC-gamma colocalized with wild-type PKC-gamma, the mutation probably acts in a dominant-negative manner on wild-type PKC. Despite normal locomotion in their home cage, 1-week-old but not 1-month-old *PRKCG*/S119P mutants had rotorod deficits.

SCA15

SCA15 is due to autosomal dominant deletions of *ITPR1* located on chromosome 3 and encoding inositol 1,4,5-triphosphate receptor 1, permitting calcium release from intracellular stores [87, 175, 176]. SCA15 causes a relatively pure cerebellar syndrome particularly affecting the vermis and marked by ataxia, intention tremor, and nystagmus [177, 178].

A targeted *Itpr1* null mutation led to ataxia and tonic or tonic–clonic seizures [88]. In addition, two spontaneous

murine mutants with *Itpr1* deletions have been discovered. The *opisthotonos* (*opt*) mouse is characterized by low inositol 1,4,5-trisphosphate receptor 1 levels, abnormal calcium responses in Purkinje cells, ataxia, and convulsions [89]. A second spontaneous deletion of *Itpr1* also decreases inositol 1,4,5-triphosphate receptor 1 levels in Purkinje cells and causes ataxia [87].

SCA17

SCA17 is an autosomal dominant disorder caused by over 43 CAG repeats in *TBP* located on chromosome 6 and encoding the TATA-binding protein, a transcription factor for many genes [179, 180]. SCA17 is characterized by ataxia, nystagmus, dystonia, and, unlike other SCA diseases, prominent neuropsychiatric signs and dementia [181].

SCA17 murine models were reviewed [182]. Mice were generated with the *TBP*/Q transgene containing 109 or 69 CAG repeats driven by the *Pcp2* promoter [90]. *TBP*/Q109 transgenic mice sustained losses in Purkinje cells and brainstem but also basal ganglia and neocortex, leading to gait anomalies on footprint analyses, paw clasping, open-field hyperactivity, and rotorod deficits. Mutated TBP aggregates were colocalized in Purkinje cells with ubiquitin and heat shock chaperone Hsc70. Purkinje cell loss, open-field hyperactivity, and rotorod deficits were mitigated by subcutaneous injection of granulocyte-colony stimulating factor to mobilize blood progenitor cells, its receptor being expressed on Purkinje cells [90, 183]. Likewise, Purkinje cell misalignment and rotorod deficits were mitigated by intraperitoneal injection of an extract from the leaves of *Ginkgo biloba*, EGb 761 [184].

Inducible *TBP*/Q105 knockin mice were generated by replacing exon 2 of the murine *Tbp* gene with exon 2 of human *TBP* carrying 105 CAGs [91]. The stop codon is flanked by two loxP sites as a targeting vector. The floxed mice were crossed with those carrying a rat *Nes* (nestin) promoter-driven Cre transgene and the stop codon removed via Cre–loxP recombination, resulting in knockin mice which express mutant and normal *TBP* under the influence of the endogenous promoter. *TBP*/Q105 knockins exhibited nuclear aggregates in Purkinje cells, Purkinje cell loss, home-cage hypoactivity, and rotorod deficits. To induce the expression of mutated mice at different ages, floxed heterozygous *TBP*/Q105 knockin mice were crossed with CreER transgenic mice expressing a fusion protein of Cre recombinase with an estrogen receptor ligand binding site driven by the chicken *Actb* (β-actin) promoter. The intraperitoneal injection of tamoxifen, an estrogen receptor ligand, binds the Cre recombinase fusion protein and makes it enter the nucleus to act on loxP sites, removing the stop codon [185]. Tamoxifen-inducible *TBP*/Q105 knockin mice exhibited Purkinje cell loss, reduced stride length on footprint patterns, paw clasping, slower MTs on the stationary beam, and rotorod deficits. The Purkinje cell loss was mitigated by intracerebellar injection of lentivral vectors expressing mesencephalic astrocyte-derived neurotrophic factor (MANF) or after interbreeding with *MANF* transgenic mice, the latter method also improving stationary beam, paw clasping, and footprint anomalies.

In addition to murine models, a rat model of SCA17 is available with 64 CAA/CAG repeats driven by the murine *Prp* promoter [92]. *TBP*/Q64 transgenic rats displayed nuclear aggregates in granule, Purkinje, and stellate cells; Purkinje cell loss; paw clasping; and more foot-slips than wild type on the stationary beam but no effect on rotorod acquisition. This result points again to the usefulness of the stationary beam as a test to be used in conjunction with the rotorod. Relative to wild type, they also showed home-cage hyperactivity at a young age and hypoactivity at an older age, but with decreased rearing throughout.

SCA27

SCA27 is an autosomal dominant-negative disorder caused by mutations in *FGF14* located on chromosome 14 and encoding fibroblast growth factor 14, an accessory subunit of voltage-gated sodium channels [186–188]. SCA27 causes a combination of cerebellar and basal ganglia symptoms including ataxia, dysarthria, nystagmus, tremors, and dyskinesia [189]. In normal mice, *Fgf14* transcripts are expressed in cerebellar granule and dorsal striatal cells [190].

In the cerebellar slice preparation of *Fgf14* null mutants, AMPA receptor-mediated excitatory postsynaptic currents evoked by parallel fiber stimulation were lower than those of wild type [190]. *Fgf14* null mutant mice exhibited overt ataxia, dyskinesia, paw clasping, reduced grip strength, open-field hyperactivity, and slowed MT before reaching the top of an inclined screen as well as shortened latencies before falling from an inverted screen or rotorod [93, 191]. The dyskinesia appears in the form of paroxysmal forelimb clonic spasms with hyperextended hind limbs.

SCA28

SCA28 is an autosomal dominant-negative disorder caused by mutations in *AFG3L2* located on chromosome 18 and encoding part of the mitochondrial ATPase-associated protease superfamily [192, 193]. The neuropathology comprises a loss in cerebellar and brainstem volumes along with extraocular muscle atrophy [194]. SCA28 is characterized by ataxia, dysarthria, nystagmus, and ophthalmoparesis [195].

Homozygous *Afg3l2* null mutant mice die on the second postnatal week. In heterozygous *Afg3l2* null mutants, ATP synthesis in the brain is defective due to insufficient assembly of respiratory complexes I and III [196]. *Afg3l2* haploinsufficiency led to granule and Purkinje cell loss, an

impaired negative geotaxic response (turning upward on an inclined grid), limb clasping, more foot-slips than normal on the stationary beam, and rotorod deficits [94]. Purkinje cell degeneration and foot-slips diminished after interbreeding *Afg3l2* haploinsufficient mice with *Grm1* haploinsufficient mice lacking mGluR1, which prevents high calcium influx into Purkinje cells [197].

Concluding Remarks

The present overview on SCA models illustrates the methodology used by researchers to determine behavioral phenotypes of cerebellar dysfunction. The cerebellum is intrinsically linked to ataxia and deficits in motor coordination since the 1917 paper by Holmes, who described the consequences of human gunshot wounds [198]. The main function of the cerebellum is to integrate sensory input with motor output, to modulate movements, not cause them, so that lesions of this area cause neither sensory deficit (hypoesthesia, blindness, or deafness) nor paralysis.

Spontaneous cerebellar mutants are featured prominently in the "Catalog of the neurological mutants of the mouse", a 1965 monograph by Sidman et al. [199], because a new cerebellar mutation is all the easier to detect in a cage, even by uninformed laboratory personnel, as a result of the obvious lurching and swaying mice, in contrast to other neurologic signs that might go undetected or are even undetectable on casual viewing. Moreover, many mutations affecting the cerebellum are embryologically nonlethal and the mutant is not generally attacked by the nonmutant in their home cage. In a laboratory maximizing animal protection, the mutation permits a relatively long life span and the possibility of analyzing behavior from early development to old age. We pointed out the use of limb clasping [200] and myoclonic jumping [201] as additional features in phenotyping neurologic mutants, including those affecting the cerebellum. In addition to qualitative observations of mutants, the need arose to provide quantified measurements of motor coordination, among which the rotorod gained prominence after the original 1962 paper by Plotnikoff et al. [202] and the 1968 paper by Jones and Roberts [203].

As shown in the present review, the rotorod is the most common sensorimor test used to evaluate SCA models. Indeed, rotorod deficits were reported in 10 SCA models, namely SCA1 to 3, SCA5 to 8, SCA14, SCA17, and SCA27. Stationary beam deficits were described in eight SCA models, namely SCA1 to 3, SCA5, SCA6, SCA13, SCA17, and SCA27, but wire suspension deficits in only SCA3 and SCA5. SCA1, SCA2, SCA3, SCA6, SCA7, and SCA14 models showed rotorod defects without overt ataxia or anomalous footprint patterns. The reverse pattern of abnormal footprint patterns and normal rotorod performance was found only in a SCA10 model. Moreover, a SCA6 model without ataxia was deficient on the stationary beam and a SCA17 model was deficient on the stationary beam but not on the rotorod, which should promote the use of the stationary beam as a test to be used in conjunction with the rotorod.

The rotorod task may be less time-consuming than other tasks in that ataxic mice are more likely to fall early, whereas early falls sometimes occur only from the narrowest stationary beam, which may cause mutants to wrap their limbs around it to prevent a fall. In the latter case, MT and distance traveled may be used as additional measures. The limb-wrapping strategy also occurs on the suspended wire, so that MT can be added on the coat hanger version of the test. Passive rotation on the rotorod can be counteracted by removing mice from the apparatus as soon as the behavior appears and considering it akin to a fall [42]. All three tests are complimented by footprint analyses to document the existence of an ataxic gait.

The question arises as to what extent stationary beam, suspended wire, and rotorod tests are selective for a cerebellar lesion relative to lesions elsewhere in the brain. The answer is that rotorod deficits have been reported after selective lesions of cerebellar afferent or efferent regions such as the inferior olive [204] and ventrolateral thalamus [205], respectively, but also parts of the basal ganglia such as the substantia nigra pars compacta [206] or lateral pallidum [207]. Likewise, cerebellar [208, 209] or dorsostriatal [210] lesions impair stationary beam performance, though the suspended wire has been less extensively investigated [211]. Therefore, current sensorimotor tests dependent on postural control seem meant to detect a central nervous system deficit rather than a specifically cerebellar-related one.

Compliance with Ethical Standards

Conflict of Interest The authors declare that they have no conflict of interest.

Publisher's Note Springer Nature remains neutral with regard to jurisdictional claims in published maps and institutional affiliations.

References

1. Cendelin J. From mice to men: lessons from mutant ataxic mice. Cerebellum Ataxias. 2014;1:4.
2. Lalonde R, Strazielle C. Motor performance of spontaneous murine mutations with cerebellar atrophy. In: Crusio W, Gerlai R, editors. Handbook of molecular-genetic techniques for brain and behavior research (techniques in the behavioral and neural sciences), vol. 13. Amsterdam: Elsevier; 1999. p. 627–37.
3. Brooks SP, Dunnett SB. Tests to assess motor phenotype in mice: a user's guide. Nat Rev Neurosci. 2009;10:519–29.
4. Caddy KW, Biscoe TJ. Structural and quantitative studies on the normal C3H and *Lurcher* mutant mouse. Philos Trans R Soc Lond Ser B Biol Sci. 1979;287:167–201.
5. Guastavino J-M, Sotelo C, Damez-Kinselle I. Hot-foot murine mutation: behavioral effects and neuroanatomical alterations. Brain Res. 1990;523:199–210.

6. Herrup K, Mullen RJ. Regional variation and absence of large neurons in the cerebellum of the *staggerer* mouse. Brain Res. 1979;172:1–12.
7. Mullen RJ, Eicher EM, Sidman RL. *Purkinje cell degeneration*: a new neurological mutation in the mouse. Proc Natl Acad Sci U S A. 1976;73:208–12.
8. Mariani J, Crepel F, Mikoshiba K, Changeux J-P, Sotelo C. Anatomical, physiological and biochemical studies of the cerebellum from Reeler mutant mouse. Philos Trans R Soc Lond Ser B Biol Sci. 1977;281:1–28.
9. Sweet HO, Bronson RT, Johnson KR, Cook SA, Davisson MT. *Scrambler*, a new neurological mutation of the mouse with abnormalities of neuronal migration. Mamm Genome. 1996;7:798–802.
10. Zuo J, De Jager PI, Takahashi KA, Jiang W, Linden DJ, Heintz N. Neurodegeneration in *Lurcher* mutant mice caused by mutation in the delta2 glutamate receptor gene. Nature. 1997;388:769–73.
11. Takayama C, Nakagawa S, Watanabe M, Mishina M, Inoue Y. Developmental changes in expression and distribution of the glutamate receptor channel delta2 subunit according to the Purkinje cell maturation. Dev Brain Res. 1996;92:147–55.
12. Lalouette A, Guénet J-L, Vriz S. Hot-foot mutations affect the δ2 glutamate receptor gene and are allelic to *Lurcher*. Genomics. 1998;50:9–13.
13. Lalouette A, Lohof A, Sotelo C, Guénet J, Mariani J. Neurobiological effects of a null mutation depend on genetic context: comparison between two *hotfoot* alleles of the delta-2 ionotropic glutamate receptor. Neuroscience. 2001;105:443–55.
14. Matsuda S, Yuzaki M. Mutation in *hotfoot-4J* mice results in retention of δ2 glutamate receptors in ER. Eur J Neurosci. 2002;16:1507–16.
15. Kashiwabuchi N, Ikeda K, Araki K, Hirano T, Shibuki K, Takayama C, et al. Impairment of motor coordination, Purkinje cell synapse formation, and cerebellar long-term depression in GluR delta 2 mutant mice. Cell. 1995;81:245–52.
16. Lalonde R, Bensoula AN, Filali M. Rotorod sensorimotor learning in cerebellar mutant mice. Neurosci Res. 1995;22:423–6.
17. Lalonde R, Filali M, Bensoula AN, Lestienne F. Sensorimotor learning in three cerebellar mutant mice. Neurobiol Learn Mem. 1996;65:113–20.
18. Lalonde R, Botez MI, Joyal CC, Caumartin M. Motor deficits in *Lurcher* mutant mice. Physiol Behav. 1992;51:523–5.
19. Strazielle C, Krémarik P, Ghersi-Egea JF, Lalonde R. Regional brain variations of cytochrome oxidase activity and motor coordination in *Lurcher* mutant mice. Exp Brain Res. 1998;121:35–45.
20. Hilber P, Caston J. Motor skills and motor learning in *Lurcher* mutant mice during aging. Neuroscience. 2001;102:615–23.
21. Krémarik P, Strazielle C, Lalonde R. Regional brain variations of cytochrome oxidase activity and motor coordination in *hot-foot* mutant mice. Eur J Neurosci. 1998;10:2802–9.
22. Hamilton BA, Frankel WN, Kerrebrock AW, Hawkins TL, Fitzhugh W, Kusumi K, et al. Disruption of the nuclear hormone receptor ROR in *staggerer* mice. Nature. 1996;379:736–9.
23. Nakagawa S, Watanabe M, Inoue Y. Prominent expression of nuclear hormone receptor RORα in Purkinje cells from early development. Neurosci Res. 1997;28:177–84.
24. Doulazmi M, Frederic F, Capone F, Becker-Andre M, Delhaye-Bouchaud N, Mariani J. A comparative study of Purkinje cells in two *RORα* gene mutant mice: staggerer and *RORα*−/−. Dev Brain Res. 2001;127:165–74.
25. Steinmayr M, André E, Conquet F, Rondi-Reig L, Delhaye-Bouchaud N, Auclair N, et al. *Staggerer* phenotype in retinoid-related orphan receptor α-deficient mice. Proc Natl Acad Sci U S A. 1998;95:3960–5.
26. Mitsumura K, Hosoi N, Furuya N, Hirai H. Disruption of metabotropic glutamate receptor signalling is a major defect at cerebellar parallel fibre-Purkinje cell synapses in *staggerer* mutant mice. J Physiol. 2011;589:3191–209.
27. Lalonde R. Motor abnormalities in *staggerer* mutant mice. Exp Brain Res. 1987;68:417–20.
28. Deiss V, Strazielle C, Lalonde R. Regional brain variations of cytochrome oxidase activity and motor co-ordination in *staggerer* mutant mice. Neuroscience. 2000;95:903–11.
29. Fernandez-Gonzalez A, La Spada AR, Treadaway J, Higdon JC, Harris BS, Sidman RL, et al. *Purkinje cell degeneration* (*pcd*) phenotypes caused by mutations in the axotomy-induced gene, *Nna1*. Science. 2002;295:1904–6.
30. Landis SC, Mullen RJ. The development and degeneration of Purkinje cells in *pcd* mutant mice. J Comp Neurol. 1978;177:125–44.
31. Le Marec N, Lalonde R. Sensorimotor learning and retention during equilibrium tests in *Purkinje cell degeneration* mutant mice. Brain Res. 1997;768:310–6.
32. D'Arcangelo G, Miao GG, Chen S-C, Soared HD, Morgan JI, Curran T. A protein related to extracellular matrix proteins deleted in the mouse mutant reeler. Nature. 1995;374:719–23.
33. D'Arcangelo G, Homayouni R, Keshvara L, Rice DS, Sheldon M, Curran T. Reelin is a ligand for lipoprotein receptors. Neuron. 1999;24:471–9.
34. Hirotsune S, Takahara T, Sasaki N, Hirose K, Yoshiki A, Ohashi T, et al. The reeler gene encodes a protein with an EGF-like motif expressed by pioneer neurons. Nat Genet. 1995;10:77–83.
35. Hack I, Bancila M, Loulier K, Carroll P, Cremer H. Reelin is a detachment signal in tangential chain-migration during postnatal neurogenesis. Nat Neurosci. 2002;5:939–45.
36. Stanfield BB, Cowan WM. The morphology of the hippocampus and dentate gyrus in normal and *reeler* mutant mice. J Comp Neurol. 1979;185:393–422.
37. Dräger UC. Observations on the organization of the visual cortex in the *reeler* mouse. J Comp Neurol. 1981;201:555–70.
38. Schiffmann SN, Bernier B, Goffinet AM. Reelin mRNA expression during mouse brain development. Eur J Neurosci. 1997;9:1055–71.
39. Caviness VS Jr, Rakic P. Mechanisms of cortical development: a view from mutations in mice. Annu Rev Neurosci. 1978;1:297–326.
40. Lalonde R, Hayzoun K, Derer M, Mariani J, Strazielle C. Neurobehavioral evaluation of *Rel* $^{rl\text{-}Orl}$ mutant mice and correlations with cytochrome oxidase activity. Neurosci Res. 2004;49:297–305.
41. Jacquelin C, Lalonde R, Jantzen-Ossola C, Strazielle C. Neurobehavioral performances and brain regional metabolism in *Dab1*^{scm} (*scrambler*) mutant mice. Behav Brain Res. 2013;252:92–100.
42. Lalonde R, Strazielle C. Sensorimotor learning in *Dab1*^{scm} (*scrambler*) mutant mice. Behav Brain Res. 2011;218:350–2.
43. Burright EN, Clark HB, Servadio A, Matilla T, Feddersen RM, Yunis WS, et al. *SCA1* transgenic mice: a model for neurodegeneration caused by an expanded CAG trinucleotide repeat. Cell. 1995;82:937–48.
44. Fernandez-Funez P, Nino-Rosales ML, de Gouyon B, She WC, Luchak JM, Martinez P, et al. Identification of genes that modify ataxin-1-induced neurodegeneration. Nature. 2000;408:101–6.
45. Zu T, Duvick LA, Kaytor MD, Berlinger MS, Zoghbi HY, Clark HB, et al. Recovery from polyglutamine-induced neurodegeneration in conditional *SCA1* transgenic mice. J Neurosci. 2004;24:8853–61.
46. Watase K, Weeber EJ, Xu B, Antalffy B, Yuva-Paylor L, Hashimoto K, et al. A long CAG repeat in the mouse *Sca1* locus replicates SCA1features and reveals the impact of protein solubility on selective neurodegeneration. Neuron. 2002;34:905–19.

47. Lorenzetti D, Watase K, Xu B, Matzuk MM, Orr HT, Zoghbi HY. Repeat instability and motor incoordination in mice with a targeted expanded CAG repeat in the *Sca1* locus. Hum Mol Genet. 2000;9:779–85.
48. Huynh DP, Figueroa K, Hoang N, Pulst SM. Nuclear localization or inclusion body formation of ataxin-2 are not necessary for SCA2 pathogenesis in mouse or human. Nat Genet. 2000;26: 44–50.
49. Aguiar J, Fernández J, Aguilar A, Mendoza Y, Vázquez M, Suárez J, et al. Ubiquitous expression of human *SCA2* gene under the regulation of the *SCA2* self promoter cause specific Purkinje cell degeneration in transgenic mice. Neurosci Lett. 2006;392:202–6.
50. Hansen ST, Meera P, Otis TS, Pulst SM. Changes in Purkinje cell firing and gene expression precede behavioral pathology in a mouse model of SCA2. Hum Mol Genet. 2013;22:271–83.
51. Dansithong W, Paul S, Figueroa KP, Rinehart MD, Wiest S, Pflieger LT, et al. Ataxin-2 regulates RGS8 translation in a new BAC-SCA2 transgenic mouse model. PLoS Genet. 2015;11: e1005182.
52. Damrath E, Heck MV, Gispert S, Azizov M, Nowock J, Seifried C, et al. ATXN2-CAG42 sequesters PABPC1 into insolubility and induces FBXW8 in cerebellum of old ataxic knock-in mice. PLoS Genet. 2012;8:e1002920.
53. Torashima T, Koyama C, Iizuka A, Mitsumura K, Takayama K, Yanagi S, et al. Lentivector-mediated rescue from cerebellar ataxia in a mouse model of spinocerebellar ataxia. EMBO Rep. 2008;9: 393–9.
54. Goti D, Katzen SM, Mez J, Kurtis N, Kiluk J, Ben-Haïem L, et al. A mutant ataxin-3 putative-cleavage fragment in brains of Machado–Joseph disease patients and transgenic mice is cytotoxic above a critical concentration. J Neurosci. 2004;24:10266–79.
55. Ikeda H, Yamaguchi M, Sugai S, Aze Y, Narumiya S, Kakizuka A. Expanded polyglutamine in the Machado–Joseph disease protein induces cell death *in vitro* and *in vivo*. Nat Genet. 1996;13:196–202.
56. Chou AH, Yeh TH, Ouyang P, Chen YL, Chen SY, Wang HL. Polyglutamine-expanded ataxin-3 causes cerebellar dysfunction of *SCA3* transgenic mice by inducing transcriptional dysregulation. Neurobiol Dis. 2008;31:89–101.
57. Silva-Fernandes A, Costa MC, Duarte-Silva S, Oliveirac P, Botelhoa MC, Martinsa L, et al. Motor uncoordination and neuropathology in a transgenic mouse model of Machado-Joseph disease lacking intranuclear inclusions and ataxin-3 cleavage products. Neurobiol Dis. 2010;40:163–76.
58. Silva-Fernandes A, Duarte-Silva S, Neves-Carvalho A, Amorim M, Soares-Cunha C, Oliveira P, et al. Chronic treatment with 17-DMAG improves balance and coordination in a new mouse model of Machado-Joseph disease. Neurotherapeutics. 2014;11:433–49.
59. Bichelmeier U, Schmidt T, Hübener J, Boy J, Rüttiger L, Häbig K, et al. Nuclear localization of ataxin-3 is required for the manifestation of symptoms in SCA3: *in vivo* evidence. J Neurosci. 2007;27:7418–28.
60. Boy J, Schmidt T, Schumann U, Grasshoff U, Unser S, Holzmann C, et al. A transgenic mouse model of spinocerebellar ataxia type 3 resembling late disease onset and gender-specific instability of CAG repeats. Neurobiol Dis. 2010;37:284–93.
61. Ramani B, Harris GM, Huang R, Seki T, Murphy GG, Costa Mdo C, et al. A knockin mouse model of spinocerebellar ataxia type 3 exhibits prominent aggregate pathology and aberrant splicing of the disease gene transcript. Hum Mol Genet. 2015;24:1211–24.
62. Switonski PM, Szlachcic WJ, Krzyzosiak WJ, Figiel M. A new humanized ataxin-3 knock-in mouse model combines the genetic features, pathogenesis of neurons and glia and late disease onset of SCA3/MJD. Neurobiol Dis. 2015;73:174–88.
63. Boy J, Schmidt T, Wolburg H, Mack A, Nuber S, Böttcher M, et al. Reversibility of symptoms in a conditional mouse model of spinocerebellar ataxia type 3. Hum Mol Genet. 2009;18:4282–95.
64. Cemal CK, Carroll CJ, Lawrence L, Lowrie MB, Ruddle P, Al-Mahdawi S, et al. YAC transgenic mice carrying pathological alleles of the MJD1 locus exhibit a mild and slowly progressive cerebellar deficit. Hum Mol Genet. 2002;11:1075–94.
65. Perkins EM, Clarkson YL, Sabatier N, Longhurst DM, Millward CP, Jack J, et al. Loss of beta-III spectrin leads to Purkinje cell dysfunction recapitulating the behavior and neuropathology of spinocerebellar ataxia type 5 in humans. J Neurosci. 2010;30: 4857–67.
66. Stankewich MC, Gwynn B, Ardito T, Ji L, Kim J, Robledo RF, et al. Targeted deletion of betaIII spectrin impairs synaptogenesis and generates ataxic and seizure phenotypes. Proc Natl Acad Sci U S A. 2010;107:6022–7.
67. Armbrust KR, Wang X, Hathorn TJ, Cramer SW, Chen G, Zu T, et al. Mutant β-III spectrin causes mGluR1α mislocalization and functional deficits in a mouse model of spinocerebellar ataxia type 5. J Neurosci. 2014;34:9891–904.
68. Mark MD, Krause M, Boele HJ, Kruse W, Pollok S, Kuner T, et al. Spinocerebellar ataxia type 6 protein aggregates cause deficits in motor learning and cerebellar plasticity. J Neurosci. 2015;35: 8882–95.
69. Du X, Wang J, Zhu H, Rinaldo L, Lamar KM, Palmenberg AC, et al. Second cistron in *CACNA1A* gene encodes a transcription factor mediating cerebellar development and SCA6. Cell. 2013;154:118–33.
70. Watase K, Barrett CF, Miyazaki T, Ishiguro T, Ishikawa K, Hu Y, et al. Spinocerebellar ataxia type 6 knockin mice develop a progressive neuronal dysfunction with age-dependent accumulation of mutant CaV2.1 channels. Proc Natl Acad Sci U S A. 2008;105: 11987–92.
71. Jayabal S, Ljungberg L, Watt AJ. Transient cerebellar alterations during development prior to obvious motor phenotype in a mouse model of spinocerebellar ataxia type 6. J Physiol. 2017;595:949–66.
72. Unno T, Wakamori M, Koike M, Uchiyama Y, Ishikawa K, Kubota H, et al. Development of Purkinje cell degeneration in a knockin mouse model reveals lysosomal involvement in the pathogenesis of SCA6. Proc Natl Acad Sci U S A. 2012;109:17693–8.
73. Chou AH, Chen CY, Chen SY, Chen WJ, Chen YL, Weng YS, et al. Polyglutamine-expanded ataxin-7 causes cerebellar dysfunction by inducing transcriptional dysregulation. Neurochem Int. 2010;56:329–39.
74. Yvert G, Lindenberg KS, Picaud S, Landwehrmeyer GB, Sahel JA, Mandel J-L. Expanded polyglutamines induce neurodegeneration and transneuronal alterations in cerebellum and retina of *SCA7* transgenic mice. Hum Mol Genet. 2000;9:2491–506.
75. Custer SK, Garden GA, Gill N, Rueb U, Libby RT, Schultz C, et al. Bergmann glia expression of polyglutamine-expanded ataxin-7 produces neurodegeneration by impairing glutamate transport. Nat Neurosci. 2006;9:1302–11.
76. Garden GA, Libby RT, Fu YH, Kinoshita Y, Huang J, Possin DE, et al. Polyglutamine-expanded ataxin-7 promotes non-cell-autonomous Purkinje cell degeneration and displays proteolytic cleavage in ataxic transgenic mice. J Neurosci. 2002;22:4897–905.
77. Yvert G, Lindenberg KS, Devys D, Helmlinger D, Landwehrmeyer GB, Mandel J-L. SCA7 mouse models show selective stabilization of mutant ataxin-7 and similar cellular responses in different neuronal cell types. Hum Mol Genet. 2001;10:1679–92.
78. Furrer SA, Mohanachandran MS, Waldherr SM, Chang C, Damian VA, Sopher BL, et al. Spinocerebellar ataxia type 7 cerebellar disease requires the coordinated action of mutant ataxin-7

in neurons and glia, and displays non-cell-autonomous bergmann glia degeneration. J Neurosci. 2011;31:16269–78.
79. Yoo SY, Pennesi ME, Weeber EJ, Xu B, Atkinson R, Chen S, et al. SCA7 knockin mice model human SCA7 and reveal gradual accumulation of mutant ataxin-7 in neurons and abnormalities in short-term plasticity. Neuron. 2003;37:383–401.
80. Alves S, Marais T, Biferi MG, Furling D, Marinello M, El Hachimi K, et al. Lentiviral vector-mediated overexpression of mutant ataxin-7 recapitulates SCA7 pathology and promotes accumulation of the FUS/TLS and MBNL1 RNA-binding proteins. Mol Neurodegener. 2016;11(1):58.
81. He Y, Zu T, Benzow KA, Orr HT, Clark HB, Koob MD. Targeted deletion of a single Sca8 ataxia locus allele in mice causes abnormal gait, progressive loss of motor coordination, and Purkinje cell dendritic deficits. J Neurosci. 2006;26:9975–82.
82. Moseley ML, Zu T, Ikeda Y, Gao W, Mosemiller AK, Daughters RS, et al. Bidirectional expression of CUG and CAG expansion transcripts and intranuclear polyglutamine inclusions in spinocerebellar ataxia type 8. Nat Genet. 2006;38:758–69.
83. White M, Xia G, Gao R, Wakamiya M, Sarkar PS, McFarland K, et al. Transgenic mice with SCA10 pentanucleotide repeats show motor phenotype and susceptibility to seizure: a toxic RNA gain-of-function model. J Neurosci Res. 2012;90:706–14.
84. McMahon A, Fowler SC, Perney T, Akemann W, Knöpfel T, Joho RH. Allele-dependent changes of olivocerebellar circuit properties in the absence of the voltage-gated potassium channels Kv3.1 and Kv3.3. Eur J Neurosci. 2004;19:3317–27.
85. Zhang Y, Snider A, Willard L, Takemoto DJ, Lin D. Loss of Purkinje cells in the PKCgamma H101Y transgenic mouse. Biochem Biophys Res Commun. 2009;378:524–8.
86. Shuvaev AN, Horiuchi H, Seki T, Goenawan H, Irie T, Iizuka A, et al. Mutant PKCγ in spinocerebellar ataxia type 14 disrupts synapse elimination and long-term depression in Purkinje cells in vivo. J Neurosci. 2011;31:14324–34.
87. van de Leemput J, Chandran J, Knight MA, Holtzclaw LA, Scholz S, Cookson MR, et al. Deletion at *ITPR1* underlies ataxia in mice and spinocerebellar ataxia 15 in humans. PLoS Genet. 2007;3(6):e108.
88. Matsumoto M, Nakagawa T, Inoue T, Nagata E, Tanaka K, Takano H, et al. Ataxia and epileptic seizures in mice lacking type 1 inositol 1,4,5-trisphosphate receptor. Nature. 1996;379:168–71.
89. Street VA, Bosma MM, Demas VP, Regan MR, Lin DD, Robinson LC, et al. The type 1 inositol 1,4,5-trisphosphate receptor gene is altered in the *opisthotonos* mouse. J Neurosci. 1997;17:635–45.
90. Chang YC, Lin CW, Hsu CM, Lee-Chen GJ, Su MT, Ro LS, et al. Targeting the prodromal stage of spinocerebellar ataxia type 17 mice: G-CSF in the prevention of motor deficits via upregulating chaperone and autophagy levels. Brain Res. 2016;1639:132–48.
91. Huang S, Ling JJ, Yang S, Li XJ, Li S. Neuronal expression of TATA box-binding protein containing expanded polyglutamine in knock-in mice reduces chaperone protein response by impairing the function of nuclear factor-Y transcription factor. Brain. 2011;134:1943–58.
92. Kelp A, Koeppen AH, Petrasch-Parwez E, Calaminus C, Bauer C, Portal E, et al. A novel transgenic rat model for spinocerebellar ataxia type 17 recapitulates neuropathological changes and supplies in vivo imaging biomarkers. J Neurosci. 2013;33:9068–81.
93. Tempia F, Hoxha E, Negro G, Alshammari MA, Alshammari TK, Panova-Elektronova N, et al. Parallel fiber to Purkinje cell synaptic impairment in a mouse model of spinocerebellar ataxia type 27. Front Cell Neurosci. 2015;9:205.
94. Maltecca F, Magnoni R, Cerri F, Cox GA, Quattrini A, Casari G. Haploinsufficiency of *AFG3L2*, the gene responsible for spinocerebellar ataxia type 28, causes mitochondria-mediated Purkinje cell dark degeneration. J Neurosci. 2009;29:9244–54.
95. Clark HB, Orr HT. Spinocerebellar ataxia type 1-modeling the pathogenesis of a polyglutamine neurodegenerative disorder in transgenic mice. J Neuropathol Exp Neurol. 2000;59:265–70.
96. Skinner PJ, Koshy BT, Cummings CJ, Klement IA, Helin K, Servadio A, et al. Ataxin-1 with an expanded glutamine tract alters nuclear matrix-associated structures. Nature. 1997;389:971–4.
97. Clark HB, Burright EN, Yunis WS, Larson S, Wilcox C, Hartman B, et al. Purkinje cell expression of a mutant allele of *SCA1* in transgenic mice leads to disparate effects on motor behaviors, followed by a progressive cerebellar dysfunction and histological alterations. J Neurosci. 1997;17:7385–95.
98. Matilla A, Roberson ED, Banfi S, Morales J, Armstrong DL, Burright EN, et al. Mice lacking ataxin-1 display learning deficits and decreased hippocampal paired-pulse facilitation. J Neurosci. 1998;18:5508–16.
99. Shuvaev AN, Hosoi N, Sato Y, Yanagihara D, Hirai H. Progressive impairment of cerebellar mGluR signalling and its therapeutic potential for cerebellar ataxia in spinocerebellar ataxia type 1 model mice. J Physiol. 2017;595:141–64.
100. Matsuura S, Shuvaev AN, Iizuka A, Nakamura K, Hirai H. Mesenchymal stem cells ameliorate cerebellar pathology in a mouse model of spinocerebellar ataxia type 1. Cerebellum. 2014;13:323–30.
101. Nakamura K, Mieda T, Suto N, Matsuura S, Hirokazu Hirai H. Mesenchymal stem cells as a potential therapeutic tool for spinocerebellar ataxia. Cerebellum. 2015;14:165–70.
102. Chintawar S, Hourez R, Ravella A, Gall D, Orduz D, Rai M, et al. Grafting neural precursor cells promotes functional recovery in an SCA1 mouse model. J Neurosci. 2009;29:13126–35.
103. Shahbazian MD, Orr HT, Zoghbi HY. Reduction of Purkinje cell pathology in *SCA1* transgenic mice by *p53* deletion. Neurobiol Dis. 2001;8:974–81.
104. Cummings CJ, Sun Y, Opal P, Antalffy B, Mestril R, Orr HT, et al. Over-expression of inducible HSP70 chaperone suppresses neuropathology and improves motor function in *SCA1* mice. Hum Mol Genet. 2001;10:1511–8.
105. Cummings CJ, Reinstein E, Sun Y, Antalffy B, Jiang Y, Ciechanover A, et al. Mutation of the E6-AP ubiquitin ligase reduces nuclear inclusion frequency while accelerating polyglutamine-induced pathology in *SCA1* mice. Neuron. 1999;24:879–92.
106. Xia H, Mao Q, Eliason SL, Harper SQ, Martins IH, Orr HT, et al. RNAi suppresses polyglutamine-induced neurodegeneration in a model of spinocerebellar ataxia. Nat Med. 2004;10:816–20.
107. Lasagna-Reeves CA, Rousseaux MW, Guerrero-Munoz MJ, Vilanova-Velez L, Park J, See L, et al. Ataxin-1 oligomers induce local spread of pathology and decreasing them by passive immunization slows spinocerebellar ataxia type 1 phenotypes. ELife. 2015;4:e10891.
108. Cvetanovic M, Patel JM, Marti HH, Kini AR, Opal P. Vascular endothelial growth factor ameliorates the ataxic phenotype in a mouse model of spinocerebellar ataxia type 1. Nat Med. 2011;17:1445–7.
109. Watase K, Gatchel JR, Sun Y, Emamian E, Atkinson R, Richman R, et al. Lithium therapy improves neurological function and hippocampal dendritic arborization in a spinocerebellar ataxia type 1 mouse model. PLoS Med. 2007;4(5):e182.
110. Perroud B, Jafar-Nejad P, Wikoff WR, Gatchel JR, Wang L, Barupal DK, et al. Pharmacometabolomic signature of ataxia SCA1 mouse model and lithium effects. PLoS One. 2013;8(8):e70610.
111. Stucki DM, Ruegsegger C, Steiner S, Radecke J, Murphy MP, Zuber B, et al. Mitochondrial impairments contribute to spinocerebellar ataxia type 1 progression and can be ameliorated by the mitochondria-targeted antioxidant MitoQ. Free Radic Biol Med. 2016;97:427–40.

112. Gennarino VA, Singh RK, White JJ, De Maio A, Han K, Kim JY, et al. Pumilio1 haploinsufficiency leads to SCA1-like neurodegeneration by increasing wild-type ataxin1 levels. Cell. 2015;160:1087–98.
113. Alves-Cruzeiro JM, Mendonça L, Pereira de Almeida L, Nóbrega C. Motor dysfunctions and neuropathology in mouse models of spinocerebellar ataxia type 2: a comprehensive review. Front Neurosci. 2016;10:572.
114. Imbert G, Saudou F, Yvert G, Devys D, Trottier Y, Garnier JM, et al. Cloning of the gene for spinocerebellar ataxia 2 reveals a locus with high sensitivity to expanded CAG/glutamine repeats. Nat Genet. 1996;14:285–91.
115. Kiehl TR, Nechiporuk A, Figueroa KP, Keating MT, Huynh DP, Pulst SM. Generation and characterization of *Sca2* (ataxin-2) knockout mice. Biochem Biophys Res Commun. 2006;339:17–24.
116. Liu J, Tang T-S, Tu H, Nelson O, Herndon E, Huynh DP, et al. Deranged calcium signaling and neurodegeneration in spinocerebellar ataxia type 2. J Neurosci. 2009;29:9148–62.
117. Kasumu AW, Liang X, Egorova P, Vorontsova D, Bezprozvanny I. Chronic suppression of inositol 1,4,5-triphosphate receptor-mediated calcium signaling in cerebellar purkinje cells alleviates pathological phenotype in spinocerebellar ataxia 2 mice. J Neurosci. 2012;32:12786–96.
118. Chang YK, Chen MH, Chiang YH, Chen YF, Ma WH, Tseng CY, et al. Mesenchymal stem cell transplantation ameliorates motor function deterioration of spinocerebellar ataxia by rescuing cerebellar Purkinje cells. J Biomed Sci. 2011;18:54.
119. Kawaguchi Y, Okamoto T, Taniwaki M, Aizawa M, Inoue M, Katayama S, et al. CAG expansions in a novel gene for Machado-Joseph disease at chromosome 14q32.1. Nat Genet. 1994;8:221–8.
120. Padiath QS, Srivastava AK, Roy S, Jain S, Brahmachari SK. Identification of a novel 45 repeat unstable allele associated with a disease phenotype at the MJD1/SCA3 locus. Am J Med Genet B Neuropsychiatr Genet. 2005;133B:124–6.
121. Schöls L, Bauer P, Schmidt T, Schulte T, Riess O. Autosomal dominant cerebellar ataxias: clinical features, genetics, and pathogenesis. Lancet Neurol. 2004;3:291–304.
122. Coutinho P, Andrade C. Autosomal dominant system degeneration in Portuguese families of the Azores Islands. A new genetic disorder involving cerebellar, pyramidal, extrapyramidal and spinal cord motor functions. Neurology. 1978;28:703–9.
123. Stevanin G, Durr A, Brice A. Clinical and molecular advances in autosomal dominant cerebellar ataxias: from genotype to phenotype and physiopathology. Eur J Hum Genet. 2000;8:4–18.
124. Chen X, Tang TS, Tu H, Nelson O, Pook M, Hammer R, et al. Deranged calcium signaling and neurodegeneration in spinocerebellar ataxia type 3. J Neurosci. 2008;28:12713–24.
125. Colomer Gould VF. Mouse models of spinocerebellar ataxia type 3 (Machado-Joseph disease). Neurotherapeutics. 2012;9:285–96.
126. Switonski PM, Fiszer A, Kazmierska K, Kurpisz M, Krzyzosiak WJ, Figiel M. Mouse ataxin-3 functional knock-out model. NeuroMolecular Med. 2011;13:54–65.
127. Saida H, Matsuzaki Y, Takayama K, Iizuka A, Konno A, Yanagi S, et al. One-year follow-up of transgene expression by integrase-defective lentiviral vectors and their therapeutic potential in spinocerebellar ataxia model mice. Gene Ther. 2014;21:820–7.
128. Nobrega C, Nascimento-Ferreira I, Onofre I, Albuquerque D, Hirai H, Déglon N, et al. Silencing mutant ataxin-3 rescues motor deficits and neuropathology in Machado-Joseph disease transgenic mice. PLoS One. 2013a;8(1):e52396.
129. Chou AH, Yeh TH, Kuo YL, Kao YC, Jou MJ, Hsu CY, et al. Polyglutamine-expanded ataxin-3 activates mitochondrial apoptotic pathway by upregulating Bax and downregulating Bcl-xL. Neurobiol Dis. 2006;21:335–45.
130. Wang HL, Hu SH, Chou AH, Wang SS, Weng YH, Yeh TH. H1152 promotes the degradation of polyglutamine-expanded ataxin-3 or ataxin-7 independently of its ROCK-inhibiting effect and ameliorates mutant ataxin-3-induced neurodegeneration in the SCA3 transgenic mouse. Neuropharmacology. 2013;70:1–11.
131. Chou AH, Chen SY, Yeh TH, Weng YH, Wang HL. HDAC inhibitor sodium butyrate reverses transcriptional downregulation and ameliorates ataxic symptoms in a transgenic mouse model of SCA3. Neurobiol Dis. 2011;41:481–8.
132. Chou AH, Chen YL, Chiu CC, Yuan SJ, Weng YH, Yeh TH, et al. T1-11 and JMF1907 ameliorate polyglutamine-expanded ataxin-3-induced neurodegeneration, transcriptional dysregulation and ataxic symptom in the SCA3 transgenic mouse. Neuropharmacology. 2015;99:308–17.
133. Nguyen HP, Hübener J, Weber JJ, Grueninger S, Riess O, Weiss A. Cerebellar soluble mutant ataxin-3 level decreases during disease progression in spinocerebellar ataxia type 3 mice. PLoS One. 2013;8:e62043.
134. Schmidt J, Schmidt T, Golla M, Lehmann L, Weber JJ, Hübener-Schmid J, et al. In vivo assessment of riluzole as a potential therapeutic drug for spinocerebellar ataxia type 3. J Neurochem. 2016;138:150–62.
135. Shakkottai VG, do Carmo Costa M, Dell'Orco JM, Sankaranarayanan A, Wulff H, Paulson HL. Early changes in cerebellar physiology accompany motor dysfunction in the polyglutamine disease spinocerebellar ataxia type 3. J Neurosci. 2011;31:13002–14.
136. Rodriguez-Lebron E, Costa MD, Luna-Cancalon K, Peron TM, Fischer S, Boudreau RL, et al. Silencing mutant ATXN3 expression resolves molecular phenotypes in *SCA3* transgenic mice. Mol Ther. 2013;21:1909–18.
137. Nobrega C, Nascimento-Ferreira I, Onofre I, Albuquerque D, Conceição M, Déglon N, et al. Overexpression of mutant ataxin-3 in mouse cerebellum induces ataxia and cerebellar neuropathology. Cerebellum. 2013;12:441–55.
138. Dick KA, Ikeda Y, Day JW, Ranum LP. Spinocerebellar ataxia type 5. Handb Clin Neurol. 2012;103:451–9.
139. Stevanin G, Herman A, Brice A, Dürr A. Clinical and MRI findings in spinocerebellar ataxia type 5. Neurology. 1999;53:1355–7.
140. Ohara O, Ohara R, Yamakawa H, Nakajima D, Nakayama M. Characterization of a new beta-spectrin gene which is predominantly expressed in brain. Mol Brain Res. 1998;57:181–92.
141. Ishikawa K, Tanaka H, Saito M, Ohkoshi N, Fujita T, Yoshizawa K, et al. Japanese families with autosomal dominant pure cerebellar ataxia map to chromosome 19p13.1-p13.2 and are strongly associated with mild CAG expansions in the spinocerebellar ataxia type 6 gene in chromosome 19p13.1. Am J Hum Genet. 1997;61:336–46.
142. Rochester L, Galna B, Lord S, Mhiripiri D, Eglon G, Chinnery PF. Gait impairment precedes clinical symptoms in spinocerebellar ataxia type 6. Mov Disord. 2014;29:252–5.
143. Zhuchenko O, Bailey J, Bonnen P, Ashizawa T, Stockton DW, Amos C, et al. Autosomal dominant cerebellar ataxia (SCA6) associated with small polyglutamine expansions in the alpha 1A-voltage-dependent calcium channel. Nat Genet. 1997;15:62–9.
144. Ljungberg L, Lang-Ouellette D, Yang A, Jayabal S, Quilez S, Watt AJ. Transient developmental Purkinje cell axonal torpedoes in healthy and ataxic mouse cerebellum. Front Cell Neurosci. 2016;10:248.
145. Jayabal S, Ljungberg L, Erwes T, Cormier A, Quilez S, El Jaouhari S, et al. Rapid onset of motor deficits in a mouse model of spinocerebellar ataxia type 6 precedes late cerebellar degeneration. eNeuro. 2015;2(6):1–18.
146. Martin JJ. Spinocerebellar ataxia type 7. Handb Clin Neurol. 2012;103:475–91.

147. David G, Abbas N, Stevanin G, Durr A, Yvert G, Cancel G, et al. Cloning of the *SCA7* gene reveals a highly unstable CAG repeat expansion. Nat Genet. 1997;17:65–70.
148. David G, Durr A, Stevanin G, Cancel G, Abbas N, Yvert G, et al. Molecular and clinical correlations in autosomal dominant cerebellar ataxia with progressive macular dystrophy. Hum Mol Genet. 1998;7:165–70.
149. Garden AG, La Spada AR. Molecular pathogenesis and cellular pathology of spinocerebellar ataxia type 7 neurodegeneration. Cerebellum. 2008;22:138–49.
150. Yu X, Ajayi A, Boga NR, Ström AL. Differential degradation of full-length and cleaved ataxin-7 fragments in a novel stable inducible SCA7 model. J Mol Neurosci. 2012;47:219–33.
151. Ramachandran PS, Boudreau RL, Schaefer KA, La Spada AR, Davidson BL. Nonallele specific silencing of ataxin-7 improves disease phenotypes in a mouse model of SCA7. Mol Ther. 2014;22:1635–42.
152. Furrer SA, Waldherr SM, Mohanachandran MS, Baughn TD, Nguyen KT, Sopher BL, et al. Reduction of mutant ataxin-7 expression restores motor function and prevents cerebellar synaptic reorganization in a conditional mouse model of SCA7. Hum Mol Genet. 2013;22:890–903.
153. Noma S, Ohya-Shimada W, Kanai M, Ueda K, Nakamura T, Funakoshi H. Overexpression of HGF attenuates the degeneration of Purkinje cells and Bergmann glia in a knockin mouse model of spinocerebellar ataxia type 7. Neurosci Res. 2012;73:115–21.
154. Chort A, Alves S, Marinello M, Dufresnois B, Dornbierer JG, Tesson C, et al. Interferon β induces clearance of mutant ataxin 7 and improves locomotion in *SCA7* knock-in mice. Brain. 2013;136:1732–45.
155. Koob MD, Moseley ML, Schut LJ, Benzow KA, Bird TD, Day JW, et al. An untranslated CTG expansion causes a novel form of spinocerebellar ataxia (SCA8). Nat Genet. 1999;21:379–84.
156. Day JW, Schut LJ, Moseley ML, Durand AC, Ranum LPW. Spinocerebellar ataxia type 8: clinical features in a large family. Neurology. 2000;55:649–57.
157. Juvonen V, Hietala M, Päivärinta M, Rantamäki M, Hakamies L, Kaakkola S, et al. Clinical and genetic findings in Finnish ataxia patients with the spinocerebellar ataxia 8 repeat expansion. Ann Neurol. 2000;48:354–61.
158. Daughters RS, Tuttle DL, Gao W, Ikeda Y, Moseley ML, Ebner TJ, et al. RNA gain-of-function in spinocerebellar ataxia type 8. PLoS Genet. 2009;5(8):e1000600.
159. Matsuura T, Yamagata T, Burgess DL, Rasmussen A, Grewal RP, Watase K, et al. Large expansion of the ATTCT pentanucleotide repeat in spinocerebellar ataxia type 10. Nat Genet. 2000;26:191–4.
160. Zu L, Figueroa KP, Grewal R, Pulst SM. Mapping of a new autosomal dominant spinocerebellar ataxia to chromosome 22. Am J Hum Genet. 1999;64:594–9.
161. Grewal RP, Achari M, Matsuura T, Durazo A, Tayag E, Zu L, et al. Clinical features and ATTCT repeat expansion in spinocerebellar ataxia type 10. Arch Neurol. 2002;59:1285–90.
162. Rasmussen A, Matsuura T, Ruano L, Yescas P, Ochoa A, Ashizawa T, et al. Clinical and genetic analysis of four Mexican families with spinocerebellar ataxia type 10. Ann Neurol. 2001;50:234–9.
163. Teive HA, Roa BB, Raskin S, Fang P, Arruda WO, Neto YC, et al. Clinical phenotype of Brazilian families with spinocerebellar ataxia 10. Neurology. 2004;63:1509–12.
164. McFarland KN, Ashizawa T. Transgenic models of spinocerebellar ataxia type 10: modeling a repeat expansion disorder. Genes. 2012;3:481–91.
165. White MC, Gao R, Xu W, Mandal S, Lim JG, Hazra TK, et al. Inactivation of hnRNP K by expanded intronic AUUCU repeat induces apoptosis via translocation of PKCdelta to mitochondria in spinocerebellar ataxia. PLoS Genet. 2010;6:e1000984.
166. Waters MF, Minassian NA, Stevanin G, Figueroa KP, Bannister JPA, Nolte D, et al. Mutations in the voltage-gated potassium channel KCNC3 cause degenerative and developmental CNS phenotypes. Nat Genet. 2006;38:447–51.
167. Stevanin G, Dürr A. Spinocerebellar ataxia 13 and 25. Handb Clin Neurol. 2012;103:549–53.
168. Issa FA, Mock AF, Sagasti A, Papazian DM. Spinocerebellar ataxia type 13 mutation that is associated with disease onset in infancy disrupts axonal pathfinding during neuronal development. Dis Model Mech. 2012;5:921–9.
169. Irie T, Matsuzaki Y, Sekino Y, Hirai H. Kv3.3 channels harbouring a mutation of spinocerebellar ataxia type 13 alter excitability and induce cell death in cultured cerebellar Purkinje cells. J Physiol. 2014;592:229–47.
170. Joho RH, Street C, Matsushita S, Knöpfel T. Behavioral motor dysfunction in Kv3-type potassium channel-deficient mice. Genes Brain Behav. 2006;5:472–82.
171. Hurlock EC, McMahon A, Joho RH. Purkinje-cell-restricted restoration of Kv3.3 function restores complex spikes and rescues motor coordination in Kcnc3 mutants. J Neurosci. 2008;28:4640–8.
172. Hiramoto K, Kawakami H, Inoue K, Seki T, Maruyama H, Morino H, et al. Identification of a new family of spinocerebellar ataxia type 14 in the Japanese spinocerebellar ataxia population by the screening of PRKCG exon 4. Mov Disord. 2006;21:1355–60.
173. Klebe S, Durr A, Rentschler A, Hahn-Barma V, Abele M, Bouslam N, et al. New mutations in protein kinase Cgamma associated with spinocerebellar ataxia type 14. Ann Neurol. 2005;58:720–9.
174. Chen DH, Raskind WH, Bird TD. Spinocerebellar ataxia type 14. Handb Clin Neurol. 2012;103:555–9.
175. Knight MA, Kennerson ML, Anney RJ, Matsuura T, Nicholson GA, Salimi-Tari P, et al. Spinocerebellar ataxia type 15 (sca15) maps to 3p24.2-3pter: exclusion of the *ITPR1* gene, the human orthologue of an ataxic mouse mutant. Neurobiol Dis. 2003;13:147–57.
176. Marelli C, van de Leemput J, Johnson JO, Tison F, Thauvin-Robinet C, Picard F, et al. SCA15 due to large ITPR1 deletions in a cohort of 333 white families with dominant ataxia. Arch Neurol. 2011;68:637–43.
177. Storey E, Gardner RJ. Spinocerebellar ataxia type 15. Handb Clin Neurol. 2012;103:561–5.
178. Gardner RJ, Knight MA, Hara K, Tsuji S, Forrest SM, Storey E. Spinocerebellar ataxia type 15. Cerebellum. 2005;4:47–50.
179. Koide R, Kobayashi S, Shimohata T, Ikeuchi T, Maruyama M, Saito M, et al. A neurological disease caused by an expanded CAG trinucleotide repeat in the TATA-binding protein gene: a new polyglutamine disease? Hum Mol Genet. 1999;8:2047–53.
180. Nakamura K, Jeong SY, Uchihara T, Anno M, Nagashima K, Nagashima T, et al. SCA17, a novel autosomal dominant cerebellar ataxia caused by an expanded polyglutamine in TATA-binding protein. Hum Mol Genet. 2001;10:1441–8.
181. Rolfs A, Koeppen AH, Bauer I, Bauer P, Buhlmann S, Topka H, et al. Clinical features and neuropathology of autosomal dominant spinocerebellar ataxia (SCA17). Ann Neurol. 2003;54:367–75.
182. Cui Y, Yang S, Li XJ, Li S. Genetically modified rodent models of SCA17. J Neurosci Res. 2017;95:1540–7.
183. Chang YC, Lin CY, Hsu CM, Lin HC, Chen YH, Lee-Chen GJ, et al. Neuroprotective effects of granulocyte-colony stimulating factor in a novel transgenic mouse model of SCA17. J Neurochem. 2011;118:288–303.
184. Huang DS, Lin HY, Lee-Chen GJ, Hsieh-Li HM, Wu CH, Lin JY. Treatment with a *Ginkgo biloba* extract, EGb 761, inhibits

excitotoxicity in an animal model of spinocerebellar ataxia type 17. Drug Des Devel Ther. 2016;10:723–31.
185. Yang S, Huang S, Gaertig MA, Li XJ, Li S. Age-dependent decrease in chaperone activity impairs MANF expression, leading to Purkinje cell degeneration in inducible SCA17 mice. Neuron. 2014;81:349–65.
186. van Swieten JC, Brusse E, de Graaf BM, Krieger E, van de Graaf R, de Koning I, et al. A mutation in the fibroblast growth factor 14 gene is associated with autosomal dominant cerebellar ataxia. Am J Hum Genet. 2003;72:191–9.
187. Brusse E, de Koning I, Maat-Kievit A, Oostra BA, Heutink P, van Swieten JC. Spinocerebellar ataxia associated with a mutation in the fibroblast growth factor 14 gene (SCA27): a new phenotype. Mov Disord. 2006;21:396–401.
188. Laezza F, Gerber BR, Lou JY, Kozel MA, Hartman H, Craig AM, et al. The FGF14(F145S) mutation disrupts the interaction of FGF14 with voltage-gated Na+ channels and impairs neuronal excitability. J Neurosci. 2007;27:12033–44.
189. Misceo D, Fannemel M, Barøy T, Roberto R, Tvedt B, Jaeger T, et al. SCA27 caused by a chromosome translocation: further delineation of the phenotype. Neurogenetics. 2009;10:371–4.
190. Wang Q, Bardgett ME, Wong M, Wozniak DF, Lou J, McNeil BD, et al. Ataxia and paroxysmal dyskinesia in mice lacking axonally transported FGF14. Neuron. 2002;35:25–38.
191. Wozniak DF, Xiao M, Xu L, Yamada KA, Ornitz DM. Impaired spatial learning and defective theta burst induced LTP in mice lacking fibroblast growth factor 14. Neurobiol Dis. 2007;26:14–26.
192. Di Bella D, Lazzaro F, Brusco A, Plumari M, Battaglia G, Pastore A, et al. Mutations in the mitochondrial protease gene AFG3L2 cause dominant hereditary ataxia SCA28. Nat Genet. 2010;42:313–21.
193. Smets K, Deconinck T, Baets J, Sieben A, Martin JJ, Smouts I, et al. Partial deletion of AFG3L2 causing spinocerebellar ataxia type 28. Neurology. 2014;82:2092–100.
194. Politi LS, Bianchi Marzoli S, Godi C, Panzeri M, Ciasca P, Brugnara G, et al. MRI evidence of cerebellar and extraocular muscle atrophy differently contributing to eye movement abnormalities in SCA2 and SCA28 diseases. Invest Ophthalmol Vis Sci. 2016;57:2714–20.
195. Mariotti C, Brusco A, Di Bella D, Cagnoli C, Seri M, Gellera C, et al. Spinocerebellar ataxia type 28: a novel autosomal dominant cerebellar ataxia characterized by slow progression and ophthalmoparesis. Cerebellum. 2008;7:184–8.
196. Maltecca F, Aghaie A, Schroeder DG, Cassina L, Taylor BA, Phillips SJ, et al. The mitochondrial protease AFG3L2 is essential for axonal development. J Neurosci. 2008;28:2827–36.
197. Maltecca F, Baseggio E, Consolato F, Mazza D, Podini P, Young SM Jr, et al. Purkinje neuron Ca2+ influx reduction rescues ataxia in SCA28 model. J Clin Invest. 2015;125:263–74.
198. Holmes G. The symptoms of acute cerebellar injuries due to gunshot injuries. Brain. 1917;40:461–535.
199. Sidman RL, Green MC, Appel SH. Catalog of the neurological mutants of the mouse. Cambridge: Harvard University Press; 1965.
200. Lalonde R, Strazielle C. Brain regions and genes affecting myoclonus in animals. Neurosci Res. 2012;74:69–79.
201. Lalonde R, Strazielle C. Brain regions and genes affecting limb-clasping responses. Brain Res Rev. 2011;67:252–9.
202. Plotnikoff N, Reinke D, Fitzloff J. Effects of stimulants on rotarod performance of mice. J Pharm Sci. 1962;51:1007–8.
203. Jones BJ, Roberts DJ. The quantitative measurement of motor inco-ordination in naive mice using an accelerating rotarod. J Pharm Pharmacol. 1968;20:302–4.
204. Gasbarri A, Pompili A, Pacitti C, Cicirata F. Comparative effects of lesions to the ponto-cerebellar and olivo-cerebellar pathways on motor and spatial learning in the rat. Neuroscience. 2003;116:1131–40.
205. Jeljeli M, Strazielle C, Caston J, Lalonde R. Effects of ventrolateral-ventromedial thalamic lesions on motor coordination and spatial orientation in rats. Neurosci Res. 2003;47:309–16.
206. Rozas G, López-Martín E, Guerra MJ, Labandeira-García JL. The overall rotorod performance test in the MPTP-treated-mouse model of parkinsonism. J Neurosci Methods. 1998;83:165–75.
207. Jeljeli M, Strazielle C, Caston J, Lalonde R. Effects of lesions of the lateral pallidum on motor coordination, spatial learning, and regional brain variations of cytochrome oxidase activity in rats. Behav Brain Res. 1999;102:61–71.
208. Pisa M. Motor somatotopy in the striatum of rat: manipulation, biting and gait. Behav Brain Res. 1988;27:21–35.
209. Schneiderman Fish B, Baisden RH, Woodruff ML. Cerebellar nuclear lesions in rats: subsequent avoidance behavior and ascending anatomical connections. Brain Res. 1979;166:27–38.
210. Joyal CC, Meyer C, Jacquart G, Mahler P, Caston J, Lalonde R. Effects of midline and lateral cerebellar lesions on motor coordination and spatial orientation. Brain Res. 1996;739:1–11.
211. Lalonde R, Strazielle C. Brain regions and genes affecting postural control. Prog Neurobiol. 2007;81:45–60.